DIAMOND

www.climate-diamond.eu

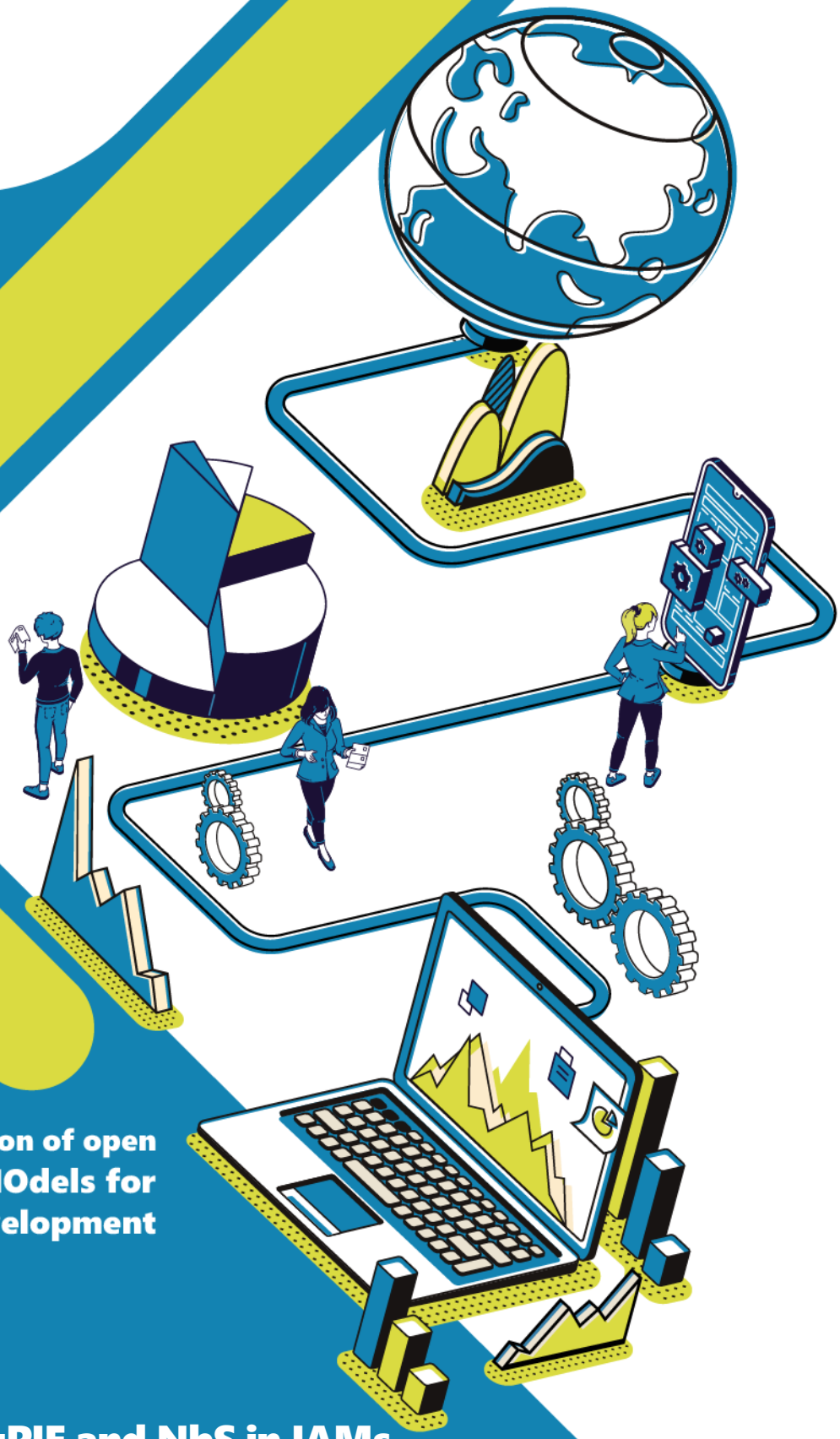

Delivering the next generation of open Integrated Assessment MOdels for Net-zero, sustainable Development

D4.2 - Expanded MAgPIE and NbS in IAMs

WP4 – Integrate & Expand

31/07/2025

Funded by the European Union

Disclaimer

Funded by the European Union. Views and opinions expressed are however those of the author(s) only and do not necessarily reflect those of the European Union or the European Climate, Infrastructure and Environment Executive Agency (CINEA). Neither the European Union nor the granting authority can be held responsible for them.

Copyright Message

This report, if not confidential, is licensed under a Creative Commons Attribution 4.0 International License (CC BY 4.0); a copy is available here: https://creativecommons.org/licenses/by/4.0/. You are free to share (copy and redistribute the material in any medium or format) and adapt (remix, transform, and build upon the material for any purpose, even commercially) under the following terms: (i) attribution (you must give appropriate credit, provide a link to the license, and indicate if changes were made; you may do so in any reasonable manner, but not in any way that suggests the licensor endorses you or your use); (ii) no additional restrictions (you may not apply legal terms or technological measures that legally restrict others from doing anything the license permits).

Grant Agreement Number	101081179		Acronym	DIAMOND
Full Title	Delivering the next generation of open Integrated Assessment MOdels for Net-zero, sustainable Development			
Topic	HORIZON-CL5-2022-D1-02			
Funding scheme	HORIZON EUROPE, RIA – Research and Innovation Action			
Start Date	December 2022	**Duration**	48 Months	
Project URL	http://www.climate-diamond.eu/			
EU Project Advisor	Silvia Vaghi			
Project Coordinator	Institute of Communications and Computer Systems - ICCS			
Deliverable	D4.2 - Expanded MAgPIE and NbS in IAMs			
Work Package	WP4 – Integrate & Expand			
Date of Delivery	**Contractual** 31/07/2025		**Actual**	31/07/2025
Nature	Report	**Dissemination**	Public	
Lead Beneficiary	Imperial College London			
Responsible Author	Maria Ioanna Malliaroudaki	**Email**	m.malliaroudaki@imperial.ac.uk	
	Imperial College London	**Phone**	-	
Contributors	Isabela Butnar, Steve Pye (UCL); Shivika Mittal (CICERO); Michael Obersteiner, Steven Lord (Oxford); George Plessias, Anastasis Giannousakis (ICCS); Marie Pied (ESMIA); Alessia Elia, Maurizio Gargiulo (E4SMA)			
Reviewer(s)	Panagiotis Fragkos, Konstantinos Koasidis (ICCS); Alessia Elia (E4SMA); Leigh Martindale (Imperial)			
Keywords	MAgPIE; Integrated Assessment Models; Land-Use; Dietary Risk Module; Nature-Based Solutions; Bioenergy; Health Impacts; Soft-linking; OMNIA; OPEN-PROM			

EC Summary Requirements

1. Changes with respect to the DoA

Considering (a) the outcomes of stakeholder interactions in the requirements and foresight workshops regarding the importance of human health, the intersection of environmental and public health policy, and biodiversity (see MS6 and D2.5) and (b) that part of what is described in the DoA on better informed economic parameters in MAgPIE, on top of Vittis et al. (2021), via detailed consideration of a wide range of options for agricultural production methods (such as land-sparing approaches that minimise land demand while delivering sustainable, affordable, and sufficient nutrition to the world's growing population) was independently implemented by the core MAgPIE team and reflected in Vittis et al. (2024), we parsed this updated economic structure directly into the DIAMOND project's version of MAgPIE (including in its links to OMNIA and OPEN-PROM, following necessary adaptations) and instead shifted our focus onto developing and linking it to both a detailed health module—allowing to capture the public health co-benefits of land-use and dietary transitions, such as reduced air pollution from biomass, improved dietary patterns, and food system changes—and a biodiversity emulator. This divergence from the DoA allowed us to integrate stakeholder feedback and external albeit relevant progress directly in our model development efforts, while putting resources into enhancing the model's capacity to evaluate societal co-benefits and trade-offs of mitigation pathways, aligning these efforts better with the DIAMOND project's broader goal of integrating well-being into IAM frameworks. No other changes with respect to the DoA are reported.

2. Dissemination and uptake

The deliverable is intended for policymakers, researchers, and the broader stakeholder community engaged in climate, land-use, food systems, and health policy. It will be particularly relevant to integrated assessment modellers and land-use specialists interested in improving the representation of agriculture, bioenergy, and nature-based solutions in climate-economy models. The addition of the dietary risk module also makes the work valuable to public health researchers and those exploring the co-benefits of sustainable food transitions. The soft-linking protocols developed for integration with OMNIA and OPEN-PROM offer practical guidance for modellers seeking to connect land-use models with IAMs in a transparent and harmonised way.

3. Short summary of results (<250 words)

Land use and food systems are essential components of climate mitigation pathways, yet their representation in integrated assessment models (IAMs) is often simplified, limiting their ability to assess nature-based solutions (NbS), sustainable agriculture, and food-health interactions. To address this, we present a set of advancements to the Model of Agricultural Production and its Impact on the Environment (MAgPIE) land-use model to improve its integration with large-scale IAMs. First, a novel dietary risk module is introduced that translates food consumption and nutritional outcomes into health impacts using Global Burden of Disease (GBD) methodologies, enabling the estimation of morbidity and mortality from diet-related risks. This adds a new dimension to IAMs by allowing exploration of co-benefits between land use, food transitions, and public health. We also improve the representation of agricultural production systems by refining cost parameters and preparing the model for a forthcoming biodiversity module. MAgPIE is then soft-linked to the OMNIA and OPEN-PROM IAMs through harmonised data exchange procedures, allowing the transfer of regionally disaggregated outputs such as land-use emissions, bioenergy supply, and NbS land allocations. These linkages enable a more robust and integrated exploration of mitigation pathways and cross-sectoral policy effects across climate, food, and health domains.

4. Evidence of accomplishment

This report.

Preface

DIAMOND will update, upgrade, and fully open six Integrated Assessment Models (IAMs) that are emblematic in scientific and policy processes, improving their sectoral and technological detail, spatiotemporal resolution, and geographic granularity. It will further enhance modelling capacity to assess the feasibility and desirability of Paris-compliant mitigation pathways, their interplay with adaptation, circular economy, and other SDGs, their distributional and equity effects, and their resilience to extremes, as well as robust risk management and investment strategies. This will be done via integration of tools and insights from psychology, finance research, behavioural and labour economics, operational research, and physical science. The project will develop a transdisciplinary scientific approach to legitimise the implementation process and co-create research questions that stretch the frontiers of climate science, as well as establish vibrant communities of practice to transparently open model enhancements and to develop capacities, thereby lowering the entrance barriers to the established IAM community.

ICCS	INSTITUTE OF COMMUNICATIONS AND COMPUTER SYSTEMS	EL
BC3	ASOCIACION BC3 BASQUE CENTRE FOR CLIMATE CHANGE - KLIMA ALDAKETA IKERGAI	ES
CESAR	KRATENA KURT	AT
CICERO	CICERO SENTER FOR KLIMAFORSKNING	NO
CYI	THE CYPRUS INSTITUTE	CY
E4SMA	ENERGY ENGINEERING ECONOMIC ENVIRONMENT SYSTEMS MODELING AND ANALYSIS SRL	IT
HOLISTIC	HOLISTIC IKE	EL
COMILLAS	UNIVERSIDAD PONTIFICIA COMILLAS	ES
ISINNOVA	ISTITUTO DI STUDI PER L'INTEGRAZIONE DEI SISTEMI (I.S.I.S) - SOCIETA'COOPERATIVA	IT
SEURECO	SEURECO SOCIETE EUROPEENNE D'ECONOMIE SARL	FR
UM	UNIVERSITEIT MAASTRICHT	NL
ESMIA	ESMIA CONSULTANTS INC.	CA
USMF	THE UNIVERSITY OF MARYLAND FOUNDATIION INC	US
UMD	UNIVERSITY OF MARYLAND	US
EPFL	ECOLE POLYTECHNIQUE FEDERALE DE LAUSANNE	CH
ETH	EIDGENOESSISCHE TECHNISCHE HOCHSCHULE ZUERICH	CH
UNIBAS	UNIVERSITAT BASEL	CH
Imperial	IMPERIAL COLLEGE OF SCIENCE TECHNOLOGY AND MEDICINE	UK
Oxford	THE CHANCELLOR, MASTERS AND SCHOLARS OF THE UNIVERSITY OF OXFORD	UK
UCL	UNIVERSITY COLLEGE LONDON	UK

Executive Summary

Land use and food systems are essential components of climate mitigation pathways, yet their representation in integrated assessment models (IAMs) is often simplified, limiting their ability to assess nature-based solutions (NbS), sustainable agriculture, and food-health interactions. This deliverable presents major improvements to the MAgPIE land-use model to enhance its integration with IAMs and support more comprehensive analysis of land use, food systems, and nature-based solutions in the context of climate change mitigation pathways.

Notably, we introduced a dietary risk module to enable the calculation and attribution of disease burden to diet risks, allowing exploration of co-benefits between land use, food transitions, and public health. Notably, MAgPIE has been enhanced, by introducing a dietary risk module that quantifies health impacts from poor diets, undernutrition, and overweight, using MAgPIE's food demand outputs in combination with global disease risk data. Dietary transitions are closely linked to land-use change required in climate change mitigation and represent one of the largest future preventable disease burdens for society. The module calculates morbidity and mortality in terms of years of life lost and years lived with disability, stratified by age, sex, and region. This allows the human capital outcomes of dietary transitions to be assessed alongside their implications for land-use change and agricultural production.

We then discuss developments in the development of a MAgPIE emulator in support of joint climate and biodiversity scenarios, better informing the economic parameters, and the inclusion of Nature based Solutions. This biodiversity module aims to link land-use outputs to ecological indicators, improving the model's ability to represent nature conservation strategies. Alongside these, parsing refinements to cost parameters and production options from the recent literature expand the economic realism of MAgPIE, allowing it to simulate a broader range of sustainable agricultural practices.

The deliverable also describes how MAgPIE has been soft-linked to the OMNIA IAM, enabling consistent transfer of data such as bioenergy availability, land-use patterns, and NbS-related land allocation. A technical mapping ensures that spatial and temporal outputs from MAgPIE are compatible with OMNIA's regional definitions and scenario logic. Nature-based solutions, including afforestation and shifts in food demand, are passed through the models in a harmonised framework that preserves internal consistency. Similarly, MAgPIE has been adapted for integration with the OPEN-PROM IAM by aligning its outputs with the model's socio-economic assumptions and scenario architecture. Bioenergy supply and prices and land-use emissions are formatted for seamless input into OPEN-PROM, and nature-based mitigation measures are consistently represented to enhance the land-use coverage of the model. These linkages allow for improved cross-model scenario analysis and pave the way for more robust policy insights.

Funded by
the European Union

Contents

1 Introduction 1
2 Enhancements in MAgPIE with a dietary risk module 2
2.1 Summary 2
2.2 Relevance 2
2.3 Module design 3
2.4 Components 4
2.4.1 Input from the MAgPIE demand module 4
2.4.2 Translation from Demand to Exposure 5
2.4.3 Diseases rate projections 7
2.4.4 Disease burden estimation 10
2.4.5 Formulas using a comparative risk methodology 11
2.4.6 Limitations in using GBD emulators 13
2.4.7 Formulas using a non-linear regression for underweight 14
2.5 Output 15
2.6 Further enhancements done in MAgPIE 16
2.6.1 Work in support of joint climate and biodiversity scenarios 16
2.6.2 Cost Modelling in DIAMOND 16
2.6.3 Representation of Nature-based Solutions in MAgPIE 17
3 Soft-Linking & Integration of Omnia and MAgPIE 18
3.1 Introduction to MAgPIE and the need to link to OMNIA 18
3.1.1 Customising MAgPIE to be compatible with OMNIA 19
3.1.2 Regional detail 19
3.1.3 Socio-economic settings 20
3.1.4 Mapping MAgPIE outputs to OMNIA inputs 21
3.1.5 Procedure for MAgPIE data extraction for OMNIA 23
3.2 Preliminary results 23
4 Soft-Linking & Integration of OPEN-PROM and MAgPIE 30
4.1 Introduction to MAgPIE and the need to link to OPEN-PROM 30
4.2 Customising MAgPIE to be compatible with OPEN-PROM 30
4.2.1 Regional Detail 30
4.2.2 Socio-economic settings 31
4.3 Mapping OPEN-PROM outputs to MAgPIE inputs 32
4.3.1 Procedure for MAgPIE data extraction for OPEN-PROM 32
4.3.2 Data Exchange Between OPEN-PROM and MAgPIE 33
4.4 Preliminary results 33
5 Conclusions & Next Steps 39
5.1 MAgPIE Dietary Risk Module Conclusions & Next Steps 39
5.2 OMNIA – MAgPIE Conclusions & Next Steps 39

Funded by the European Union

5.3 OPEN-PROM – MAgPIE Conclusions & Next Steps 39
5.4 Overall conclusions and next steps 40
References 41

Table of Figures

Figure 1. Inputs, outputs and components of a MAgPIE dietary risk module 4
Figure 2. Soft-linking between OMNIA and MAgPIE. OMNIA provides MAgPIE with the level of biomass and bioenergy demand and CO_2 prices, while MAgPIE provides costs and related GHG emissions when producing the requested amount of bioenergy under the same socio-economic scenarios. 19
Figure 3. Visual graph for the geographical representation on OMNIA regions in MAgPIE including the number of original clusters in each region. 20
Figure 4. High-level representation of biomass and bioenergy in OMNIA and MAgPIE. 21
Figure 5. Detailed representation of the MAgPIE to OMNIA mapping, including the different types of biomass and bioenergy and associated costs. For instance, 'agricultural residues' in OMNIA come from three different types of crop residues in MAgPIE, i.e. cereal straw, rice husks (fibrous residues) and other crop residues (non-fibrous residues). 22
Figure 6. Biomass feedstock and biofuel data extraction from MAgPIE for OMNIA use. 23
Figure 7. MAgPIE energy crop availability at different prices in each region, over the modelling time, exported from MAgPIE to OMNIA, in OMNIA format for SSP2 analysis. 24
Figure 8. Total bioenergy production, with 2nd generation bioenergy in green shade and 1st generation bioenergy in red shade 25
Figure 9. Regional energy crop production by biomass type, green shade denoting trees, red shade denoting grasses. 26
Figure 10. Regional crop residues available for energy production by type, blue shade denoting straw (cereal residues), green shade denoting other fibrous crop residues (e.g. rice husks), and red denoting non fibrous crop residues (e.g. corn stove) 27
Figure 11. Regional land expansion of 2nd generation energy crops (tree and grasses). 28
Figure 12. Land expansion of 2nd generation energy crops: trees (green shade) and grasses (red shade) in different biomass prices scenarios. 28
Figure 13. Cumulative land use change emissions in different biomass prices scenarios showing CO_2 sequestration by natural regrowth (orange shade) and timber plantations (brown shade), and GHG emissions from wood harvest (dark red), soil emissions (dark green), peatland loss (blue), other land conversion (green) and deforestation (red shade). 29
Figure 14. Geographical mapping of OPEN-PROM regions in MAgPIE regions including the number of original clusters in each region and their respective ISO3 code. 31
Figure 15. Geographical representation of OPEN-PROM regions in MAgPIE including the number of original clusters in each region 31
Figure 16. Bioenergy Price | Final Energy SSP2- NPi scenario. 34
Figure 17. Bioenergy Price | Final Energy SSP2- 2C scenario. 34
Figure 18. Bioenergy Price | Final Energy SSP2- 1p5C. 35
Figure 19. CO_2 Emissions from the AFOLU sector in the SSP2- NPi scenario. 35
Figure 20. CO_2 Emissions from the AFOLU sector in the SSP2- 2C scenario. 36
Figure 21. CO2 Emissions from the AFOLU sector in the SSP2- 1p5C scenario. 36

Funded by the European Union

Figure 22. CO_2 Emissions from the AFOLU sector in the alternative climate policy scenarios for Germany (DEU). 37
Figure 23. Bioenergy Price | Final Energy between the SSP2 scenarios for USA. 38

Table of Tables

Table 1. 15 dietary intake quantities associated to human disease outcomes from over and under consumption used in the 2017 Global Burden of Disease (GBD). 5
Table 2. Matrix mapping MAgPIE food demand categories to GBD dietary risk exposure categories 7
Table 3. Quantities associated with impact - health outcomes related to dietary intake as used by the GBD 2017 study. 8
Table 4. Dietary risks and related disease outcomes as in the GBD 2017 study (Stanaway et al., 2018). Some risk-disease relationships used the same relative risk function for morbidity and mortality and are listed here as 'same'. However, a few disease outcomes (for example a diet low in nuts and seeds associated with an ischemic heart disease) had individual relative risk functions for morbidity and mortality. To indicate this, they are referred to as 'differing'. 8
Table 5. Exposure inputs and categories for estimation. 10
Table 6. Geographical representation on OMNIA regions in MAgPIE including the number of original clusters in each region 20

Funded by
the European Union

1 Introduction

Land use and food systems play a central role in climate mitigation, biodiversity protection, and human wellbeing. However, in many integrated assessment models (IAMs) their representation remains limited, with key dynamics such as agricultural production methods, dietary shifts, and nature-based solutions (NbS) often being overlooked. This deliverable outlines a set of targeted enhancements to the Model of Agricultural Production and its Impact on the Environment (MAgPIE) framework to address these gaps and support robust integration with IAMs used within the DIAMOND project. Deliverable D4.2 presents major improvements to the MAgPIE land-use model to enhance its integration with energy-economic IAMs and support more comprehensive analysis of land use, food systems, and nature-based solutions.

Aiming to enhance MAgPIE, a dietary risk module was introduced that quantifies health impacts from poor diets, undernutrition, and overweight, using MAgPIE's food demand outputs in combination with global disease risk data. The module calculates morbidity and mortality in terms of years of life lost and years lived with disability, stratified by age, sex, and region. This allows the effects of dietary transitions to be assessed alongside land-use change and agricultural production. We also report on advancements to work that is also underway on a biodiversity module that will link land-use outputs to ecological indicators, improving the model's ability to represent nature conservation strategies. Alongside these, refinements to cost parameters and production options expand the economic realism of MAgPIE, allowing it to simulate a broader range of sustainable agricultural practices.

The deliverable also describes how MAgPIE has been soft-linked to the OMNIA IAM, enabling consistent transfer of data such as bioenergy availability, land-use patterns, and NbS-related land allocation. A technical mapping ensures that spatial and temporal outputs from MAgPIE are compatible with OMNIA's regional definitions and scenario logic. Nature-based solutions, including afforestation and shifts in food demand, are passed through the models in a harmonised framework that preserves internal consistency. Similarly, MAgPIE has been adapted for integration with the OPEN-PROM IAM by aligning its outputs with the model's socio-economic assumptions and scenario architecture. Bioenergy and land-use emissions are formatted for seamless input into OPEN-PROM, and nature-based mitigation measures are consistently represented. These linkages allow for improved cross-model scenario analysis and pave the way for more robust policy insights.

By expanding the scope of MAgPIE to include human health and biodiversity dimensions, and by ensuring interoperability with IAMs, this deliverable strengthens the capacity of the DIAMOND modelling ecosystem to assess the multifaceted impacts of climate and food policies. The developments outlined here open the door for more detailed and policy-relevant scenario analysis and support the inclusion of food, land, and health linkages in global sustainability assessments.

Funded by
the European Union

2 Enhancements in MAgPIE with a dietary risk module

2.1 Summary

A proposed enhancement to The Model of Agricultural Production and its Impact on the Environment (MAgPIE) is the addition of a dietary risk estimation module. The module (Figure 1) is:

- taking the outputs from the existing MAgPIE dietary demand module, and exogenous macro-economic parameters,
- and translate them into the key inputs of the dietary risk public health emulators, which are the exposure variables to underweight, overweight, and dietary composition, and the overall trajectory of disease burden from neo-plasms, cardiovascular disease, and diabetes type II.

From the exposure variables, an emulator inside the module calculates a population attributable fraction (PAF), which is the proportion of an overall disease burden attributable to the exposure. The dietary risk module outputs the overall disease burden measured in years of life lost to mortality or morbidity stratified by three age groups and by sex. The module output of population disease burden attributable to exposure to dietary risks adds to the fundamental outputs of MAgPIE, or it can be integrated in downstream modelling as a measure of labour impact. For example, in computable general equilibrium (CGE) modelling, coupling the labour impact can be incorporated into economic output calculations combining labour and capital and thereby energy demand. The output should be interpreted as the annual incident rate of mortality or morbidity associated to exposure.

2.2 Relevance

The Global Burden of Disease (GBD) study identifies dietary risks—poor diet composition, high BMI (overweight), and undernutrition—as major contributors to the global disease burden, surpassing air pollution and heat stress in preventable deaths and disability-adjusted life years (DALYs).

Poor diets caused 11 million deaths and 257 million DALYs in 2017. Deficiencies in fruits, vegetables, whole grains, nuts, and seeds are more harmful than excesses in trans fats or sugary foods (Afshin et al., 2019). Overweight (High BMI) is linked to heart disease, stroke and diabetes. From 1990 to 2017, related deaths and DALYs more than doubled, reaching 4.7 million deaths and 148 million DALYs in 2017. Undernutrition in the form of protein energy malnutrition (PEM), especially affects children under 5 and the elderly, leading to 1.5 million deaths and 62 million DALYs in 2019 (Murray et al., 2020). Combined exposure to malnutrition is associated to over annual rates of 14 million preventable deaths and 400 million DALYS.

Air pollution is a significant contributor to global disease burden (Evangelopoulos et al., 2020). It is linked to cardiovascular and respiratory diseases, cancers, and other conditions. In the 2017 study, the burden is equivalent to 7 million deaths and 213 million disability-adjusted life years (DALYs) (Global Burden of Disease Collaborative Network, 2018).

Heat stress caused 150,000 deaths and 3.4 million DALYs in 2019, disproportionately affecting males, the elderly, and low-income regions (Murray et al., 2020).

Heat stress and air pollution can be intensified by climate change and land-use changes. However, agricultural productivity, development and incomes could also be affected greatly by climate change, impacting food security and increasing exposure to dietary risks. Integrated modelling should account for how climate policies, land use, and economic shifts affect food systems and health outcomes. A dietary risks module attached to the dynamic recursive land-use allocation model MAgPIE (Dietrich et al., 2019) would enable more completely capturing human

Funded by the European Union

risks resulting from changes in agricultural productivity and development to under future scenario studies.

The outputs from a dietary risk module would be direct information about disease burdens which can be compiled with integrated model outputs on air pollution, and it can be used coupled with other IAMs to estimate a labour loss component.

2.3 Module design

Figure 1 illustrates the schematic of a proposed MAgPIE module that integrates a GBD emulator. Exogenous inputs and endogenous results from MAgPIE, particularly from the MAgPIE demand module, can be fed into the module. The calculation of the disease burden output, in years of life lost to premature death (YLL) and to preventable morbidity (YLD) is performed by a GBD emulator.

The GBD emulator performs the comparative risk calculation (Murray et al., 2003). Formulas for the calculation are indicated in the section below. The calculation requires internal parameters, inputs of exposure (received from another component of the dietary module, see Figure 1), and inputs of total population disease rates (received from another component of the dietary module). Internal parameters that can be customised are the threshold of minimum exposure (TMREL) above or below which exposure does not increase risk, and the relative risk parameters (RR), which connect exposure to increased risk of disease outcomes. The relative risk parameters are derived from the Global Burden of Disease study hosted by IHME at the University of Washington, available in the supplemental to (Afshin et al., 2019). See also the limitations section below. Custom modification of TMREL and RR, which together define relative risk functions which are integrated over population distributions of exposure, would represent alternative specification of vulnerability to exposure to dietary risks. Comparative decreases in vulnerability of public health to dietary risk exposure over future scenarios due to technology is a possible reason for modifying the internal parameters.

The GBD emulator calculates population attributable fractions (PAFs) from relative risk and exposure. These fractions are multiplied by the total disease burden, such as the total premature deaths in a population in an age and sex bracket, to form the attributable disease burden from the exposure. The attributable disease burden is the output of the module. Exposure, in the form of population distributions of intake across 13 dietary risk categories, is estimated assuming a translation component within the module and fed to the emulator. Total disease rate projections are based upon adjustments from historical projections (Vollset et al., 2024). Historical disease rates are extrapolated by the GBD from national cause of death records.

Exposure and total disease burden are adjusted using the inputs from MAgPIE on dietary demand and demographic factors. If the internal relative risk factors are left constant, then exposure and the total disease burden are the components which are dynamically updated by the connection to MAgPIE.

Funded by
the European Union

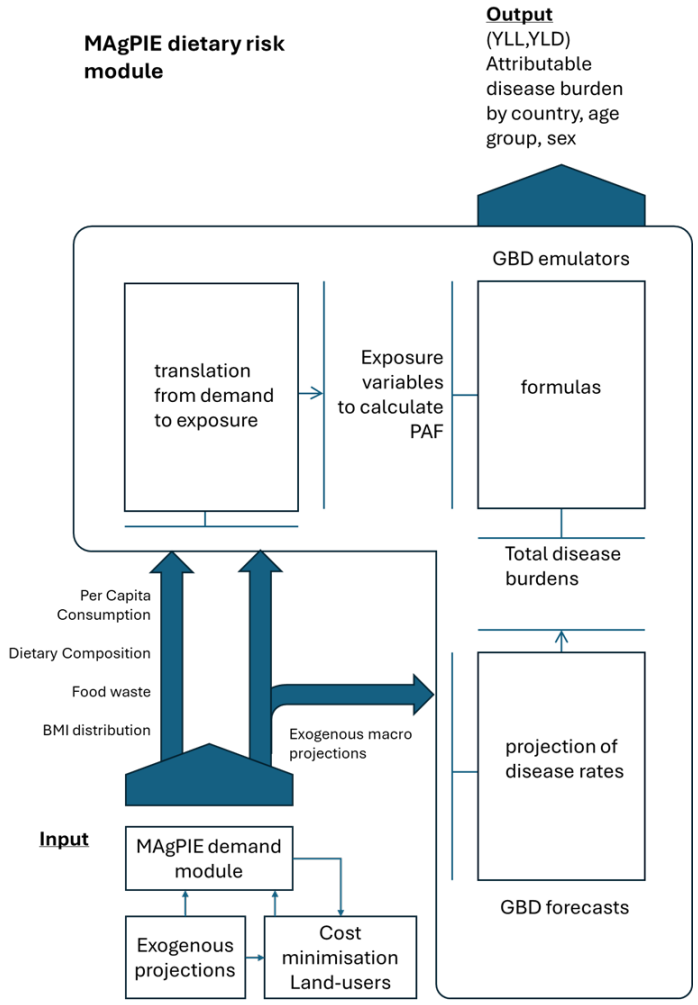

Figure 1. Inputs, outputs and components of a MAgPIE dietary risk module

2.4 Components

The proposed module's inputs, outputs and components are described in this section.

2.4.1 Input from the MAgPIE demand module

The outputs of the demand module in MAgPIE at country level are:

- **Food Demand (vm_dem_food)**: This is the total demand for various agricultural products, measured in million tons of dry matter per year (10^6 tDM/yr)
- **Per Capita Consumption (pm_kcal_pc_initial)**: This indicates the initial per capita consumption of food before any price shocks, measured in kilocalories per capita per day (kcal/capita/day)
- **Anthropometric Parameters**: Body height, weight distribution, and physical activity levels by age and sex
- **Dietary Composition**: Detailed outputs on the intake of different food groups, including livestock products, empty calories (sugar, oil, and alcohol), fruits, vegetables, nuts, and staple calories (kcal/capita/day)
- **Food Waste**: Estimates of food waste levels (10^6 tDM/yr)

Funded by the European Union

- **BMI Distribution**: The distribution of Body Mass Index (BMI) by age and sex into underweight, normal, overweight and obese (discrete distribution for BMI < 18.5, 18.5 <= BMI < 25, 25 <= BMI < 30, BMI >= 30).

2.4.2 Translation from Demand to Exposure

The MAgPIE demand module provides a population per capita calorie consumption envelope, some physical activity levels by age and sex, and some dietary composition breakdowns by several broad categories. The food demand component of agricultural products provides a more detailed breakdown in the composition of what is grown, but there are known challenges in translating what is grown into what is consumed, beyond levels of food waste.

The outputs of the demand module do not match the exposure variables of the GBD dietary composition model (Table 1) either in intake food group or nutrient detail or in disaggregation into age and sex groups in the population. Therefore, translation from the demand module to exposure input is required.

For the first version of dietary risk module the translation component uses an adjustment approach. Estimates for all exposure variables are available at the necessary detail for all countries and age-sex sub-populations from current (2021) GBD data that is available. Therefore, the adjustment approach uses the demand module outputs and demographic factors to proportionally adjust historical intake. Dynamic adjustments over 5-year time steps therefore lead to proportionally adjusted trajectories from the GBD baseline.

Exposure to over and under consumption in terms of dietary composition in the GBD study is measured by distributions of per capita adult dietary intake exceeding or below, respectively, an optimal level of intake for each dietary risk category (Table 1) (Stanaway et al., 2018). The distributions are estimated, and imputed from statistical modelling, from national surveys and 24 dietary recall studies by the GBD study.

Table 1. 15 dietary intake quantities associated to human disease outcomes from over and under consumption used in the 2017 Global Burden of Disease (GBD).

Dietary intake quantity	Intake unit	Dietary risk factor	Optimal Level of Intake (in intake units)
Fruit (excl. fruit juice)	grams per day per capita (g/capita/day)	Diet low in fruit	250 (200-300)
Vegetables (excl. starchy vegetables)	grams per day per capita (g/capita/day)	Diet low in vegetables	360 (290-430)
Whole grains	grams per day per capita (g/capita/day)	Diet low in wholegrains	125 (100-150)
Legumes	grams per day per capita (g/capita/day)	Diet low in legumes	60 (50-70)
Nuts and seeds	grams per day per capita (g/capita/day)	Diet low in nuts and seeds	21 (16-25)
Milk	grams per day per capita (g/capita/day)	Diet low in milk	435 (350-520)
Fibre	grams per day per capita (g/capita/day)	Diet low in fibre	24 (19-28)
Calcium	grams per day per capita (g/capita/day)	Diet low in calcium	1.25 (1.00-1.50)
Red meat (excl. processed)	grams per day per capita (g/capita/day)	Diet high in red meat	23 (18-27)

Funded by the European Union

Preserved / processed meat	grams per day per capita (g/capita/day)	Diet high in processed meat	2 (0-4)
Omega-3 fatty acids (from seafood consumption)	grams per day per capita (g/capita/day)	Diet low in omega-3 fatty acids	0.25 (0.20-0.30)
Omega-6 polyunsaturated fatty acids	% of total kcal intake per capita per day	Diet low in omega-6 polyunsaturated fatty acids	11 (9-13)
Trans Fat	% of total kcal intake per capita per day	Diet high in trans fatty acids	0.5 (0.0-1.0)
Sugar-sweetened beverage (incl. carbonated beverages, sodas, energy drinks, sweetened fruit drinks excl. 100% fruit and vegetable juices)	grams per day per capita (g/capita/day) of beverages with ≥50 kcal per 226.8g serving	Diet high in sugar-sweetened beverages	3 (0-5)
Sodium	24h urinary sodium in grams per day per capita (g/capita/day)	Diet high in sodium	3 (1-5)

Note: Summary of Table on p. 3 in (Stanaway et al., 2018). For risk from low intake, the optimal level of intake indicates the level below which intake is associated to preventable disease outcomes. For risk from high intake, the optimal level of intake indicates the level above which intake is associated to preventable disease outcomes. The intervals above, or below respectively, optimal intake are called the TMREL intervals. Public health models using population attributable fractions attribute the additional disease outcomes due to distributions of adult population dietary intake supported outside the TMREL interval. Optimal levels of intake are uncertain, and the range from (Stanaway et al., 2018) given in brackets for optimal intake is used in uncertainty modelling.

Dietary intake trajectories are projected from 2020 to 2050 using proportional adjustment of present intake obtained from (Bodirsky et al., 2020). To operationalise the adjustment approach, a matrix was constructed to translate demand for agricultural products, provided by the MAgPIE model into the dietary risk exposure variables specified by the GBD framework (Table 2). Demand, provided in 5-year time steps, includes projections for three broad food demand categories. These categories do not directly align with the GBD dietary risk exposures. The matrix reconciles differences in food group definitions between the two systems, and is applied consistently across all time-points. As part of this approach, proportional change factors were calculated by comparing demand at each future time-point to the baseline year, for each category. These factors represent relative shifts in per capita food demand. Once mapped, these factors were used to scale the corresponding GBD baseline mean exposures, resulting in adjusted intake values for each dietary risk. This allowed for the generation of projected exposure inputs by country, age group, sex, and time-point, aligned with demand trends.

To calculate the proportional change in per capita demand for MAgPIE food group *g*, in country *c*, at time *t*, relative to the 2020 baseline, the following formula is used:

$$\propto_{gct} = \frac{D_{gct}}{D_{gc,2020}} \quad (1)$$

where, D_{gct} and $D_{gc,2020}$ are per capita demand values for year *t* and 2020 respectively.

To calculate the mean exposure μ to a dietary risk factor *j*, in country *c*, age group *a*, sex *s*, and year *t*, based on proportional changes in food demand *g*, we use:

$$\mu_{jasc,t} = \mu_{jasc,2020} \cdot \propto_{g=c(j)t} \quad (2)$$

Funded by the European Union

where, $\propto_{g=c(j)t}$ denotes the MAgPIE food demand category *g* corresponding to GBD risk category *j* in Table 2.

Table 2. Matrix mapping MAgPIE food demand categories to GBD dietary risk exposure categories

MAgPIE food demand categories	GBD dietary risk factors
Demand for animal source foods	Diet high in red meat
Demand for animal source foods	Diet low in milk
Demand for animal source foods	Diet low in calcium
Demand for empty calories	Diet high in processed meat
Demand for empty calories	Diet high in sodium
Demand for empty calories	Diet high in sugar-sweetened beverages
Demand for empty calories	Diet high in trans fatty acids
Demand for vegetables, fruits and nuts	Diet low in fiber
Demand for vegetables, fruits and nuts	Diet low in fruits
Demand for vegetables, fruits and nuts	Diet low in legumes
Demand for vegetables, fruits and nuts	Diet low in nuts and seeds
Demand for vegetables, fruits and nuts	Diet low in whole grains
Demand for vegetables, fruits and nuts	Diet low in vegetables

The MAgPIE demand module can also output food supply in kcal/capita/day for a range of aggregate food groups, such as fruits, vegetables and nuts, dairy, and monogastric meat, with or without food waste management. To convert food supply into dietary exposures compatible with GBD definitions, a machine learning approach could also be used, as an alternative to the adjustment approach mentioned above or as a complement to understand proportional shifts within groups. In this approach, the food supply output is first harmonised to FAO Food Balance Sheet categories. This can then be used to train a random forest algorithm on historical relationships between supply and GBD dietary intake data. This machine learning model can be powerful because it captures high-dimensional, non-linear relationships between food supply and dietary intake. Furthermore, it also incorporates purchasing levels of ultra-processed foods, development indicators such as HDI and income GNI (Paulus, E., & Lord, S., 2022). Estimation of marginal damage costs from consumption related health risks (Documentation of the SPIQ-FS Dataset Version 0, Annex A; Lord, 2021). In this way, some projected income and demographic changes could be used to project forward the relationship between food supply and dietary intake. Such a model was used within studies of sustainable food system pathways for the FAO, (Vittis et al., 2024). However, the model is limited by its reliance on historical patterns, which may not hold under future food system changes, hence our initial preference on the approach described above.

Exposure to high or low BMI (overweight or underweight, respectively) is easier to adjust than dietary composition, since the MAgPIE demand module provides an estimate of the proportion of the population above BMI 30 or below BMI 18.5. The GBD distributions based on 2021 distributions of BMI are adjusted to exactly represent the same proportional changes in the percentages of the populations above BMI 30 (the right tail of the distribution) or below BMI 18.5 (the left tail of the distribution), in age-sex subpopulation BMI distributions, respectively.

2.4.3 Diseases rate projections

Disease outcomes attributable to dietary intake can be summarised into three different categories (Table 3). The largest contribution are cardiovascular diseases of which intracerebral haemorrhage, ischaemic heart disease, ischaemic stroke and subarachnoid haemorrhage were included in the GBD study. The second largest group includes diabetes mellitus type II as well as kidney diseases, which were not further specified in the GBD. Furthermore, the occurrence of neoplasms can be influenced by food consumption including the occurrence of colon and rectum cancer, stomach cancer, oesophageal cancer, larynx cancer, lip and oral cavity cancer, nasopharynx cancer, other pharynx cancer, as well as tracheal, bronchus, and lung cancer.

Funded by
the European Union

Table 3. Quantities associated with impact - health outcomes related to dietary intake as used by the GBD 2017 study.

Disease category	Diseases associated with dietary intake
Cardiovascular diseases	Ischaemic heart disease
	Ischaemic stroke
	Intracerebral haemorrhage
	Subarachnoid haemorrhage
Neoplasms	Lip and oral cavity cancer
	Nasopharynx cancer
	Other pharynx cancer
	Oesophageal cancer
	Stomach cancer
	Colon and rectum cancer
	Larynx cancer
	Tracheal, bronchus, and lung cancer
Diabetes and kidney diseases	Diabetes mellitus type 2

Every risk is associated with some, but not necessarily all metabolic mediators of diseases, which can be summarised as related to influences on the body mass index, the total serum cholesterol, the fasting plasma glucose, as well as the systolic blood pressure. Those mediators influence the vulnerability of the human body to the dietary related diseases as well as their likelihood. Table 4 gives an overview over which risk factors are associated with which disease outcomes. Furthermore, this risk is determined by factors such as age, sex, or socio-economic status.

Table 4. Dietary risks and related disease outcomes as in the GBD 2017 study (Stanaway et al., 2018). Some risk-disease relationships used the same relative risk function for morbidity and mortality and are listed here as 'same'. However, a few disease outcomes (for example a diet low in nuts and seeds associated with an ischemic heart disease) had individual relative risk functions for morbidity and mortality. To indicate this, they are referred to as 'differing'.

Risk	Disease	Morbidity/ Mortality
Diet low in fruits	Lip and oral cavity cancer	Same
	Nasopharynx cancer	Same
	Other pharynx cancer	Same
	Oesophageal cancer	Same
	Larynx cancer	Same
	Tracheal, bronchus, and lung cancer	Same
	Ischemic heart disease	Same
	Ischemic stroke	Same
	Intracerebral haemorrhage	Same
	Subarachnoid haemorrhage	Same
	Diabetes mellitus type 2	Same
Diet low in vegetables	Ischemic heart disease	Same
	Ischemic stroke	Same
	Intracerebral haemorrhage	Same

	Subarachnoid haemorrhage	Same
Diet low in legumes	Ischemic heart disease	Same
Diet low in whole grains	Ischemic heart disease	Same
	Ischemic stroke	Same
	Intracerebral haemorrhage	Same
	Subarachnoid haemorrhage	Same
	Diabetes mellitus type 2	Same
Diet low in nuts and seeds	Ischemic heart disease	Differing
	Diabetes mellitus type 2	Same
Diet low in milk	Colon and rectum cancer	Same
Diet high in red meat	Colon and rectum cancer	Same
	Diabetes mellitus type 2	Same
	Colon and rectum cancer	Same
	Ischemic heart disease	Same
	Diabetes mellitus type 2	Same
Diet low in fiber	Colon and rectum cancer	Same
	Ischemic heart disease	Same
Diet low in calcium	Colon and rectum cancer	Same
Diet low in seafood omega-3 fatty acids	Ischemic heart disease	Differing
Diet low in polyunsaturated fatty acids	Ischemic heart disease	Same
Diet high in trans fatty acids	Ischemic heart disease	Same
Diet high in sodium	Stomach cancer	Same
Diet high in sugar-sweetened beverages	Ischemic heart disease	Same
	Diabetes mellitus type 2	Same

The original GBD study also included four additional health outcomes related to a 'Diet high in sodium' namely ischemic heart disease, ischemic stroke, intracerebral haemorrhage, and subarachnoid haemorrhage. However, the risk estimation for those factors was done differently in the GBD study to the other factors listed above, and the exact calculation method of these dependencies was not explained in the GBD 2017 documentation. Therefore, DALYs related to this risk-disease combination were excluded from our calculations.

Upon request, the Institute for Health Metrics and Evaluation (IHME) at the University of Washington provides mean projections of Years of Life Lost (YLL) and Years Lived with Disability (YLD) for each country, disease outcome, and age group for the years 2022 to 2050. Since the GBD dietary composition model requires sex-disaggregated inputs, sex-specific projections were derived by redistributing total YLL and YLD values using male and female proportions from GBD 2021 estimates. Therefore, only the population sex ratio change in the exogenous population projections for a MAgPIE study will create changes in the ratio of disease burden between sexes in a fixed age group.

To ensure alignment with the demographic projections used in the MAgPIE framework, disease burden estimates from the IHME were rescaled accordingly. First, per capita disease rates for disease outcome o were calculated for each country c, age group a, sex s and year t by dividing GBD YLL and YLD projections by the corresponding GBD population estimates.

$$Mortality\ per\ capita_{ocast}^{GBD} = \frac{YLL_{cast}^{GBD}}{Population_{cast}^{GBD}} \quad (3)$$

$$Morbidity\ per\ capita_{ocast}^{GBD} = \frac{YLD_{cast}^{GBD}}{Population_{cast}^{GBD}} \quad (4)$$

These rates were then scaled to match MAgPIE population projections for the same subgroups and time periods.

$$YLL_{oasct} = Population_{cast}^{\mathrm{MAgPIE}} . Mortality\ per\ capita_{ocast}^{GBD} \quad (5)$$

$$YLD_{oasct} = Population_{cast}^{\mathrm{MAgPIE}} . Morbidity\ per\ capita_{ocast}^{GBD} \quad (6)$$

This was done to ensure that future disease burden projections remain consistent across the two frameworks.

2.4.4 Disease burden estimation

As described in Milestone MS7 report of DIAMOND, the ability of the MagPIE demand module to separate BMI distribution inputs from dietary composition enables the calculation of underweight, overweight, and weight-normalised dietary composition components.

Diets low in fruit, vegetables, nuts, wholegrains, calcium and protective fats, and diets high in sodium, sugar-sweetened beverages, saturated fats and processed meat have been associated with preventable morbidity and mortality in national populations from neoplasms (cancers), cardiovascular disease and type-2 diabetes (Afshin et al., 2019). Excessively-high caloric diets and the eating of foods causing the impairment of metabolic functioning have contributed to the human burden of disease through high BMI (Dai et al., 2020). Attribution of the burden of disease from high BMI to agrifood systems is debated in literature due to cofactors such as physical activity. The Global Burden of Disease Models developed and maintained by the Institute of Health Metrics and Evaluation (IMHE) from 2017, 2019, and 2021 (referred to as GBD2017, GBD 2019, and GBD 2021 respectively) studies have 15 exposure variables for 15 individual categories of dietary composition risk and 1 exposure variable for high BMI. The exposure variables of dietary composition in GBD models are intended to weight normalised and are meant to represent dietary composition in the population normalized to 2100 calories. However, the burden of preventable morbidity and mortality from high BMI and the dietary composition categories, and within the dietary composition categories, are not mutually exclusive and is not independently additive. Only 13 of the 15 GBD exposure variables are used to avoid double counting, as mentioned in the limitations below.

Table 5. Exposure inputs and categories for estimation.

Category	Subcategory	Exposure	Distribution	Adjustment
Overweight		High BMI	Population above BMI 30	Scale
Dietary composition	Diets high in processed foods and additives	Diet high in processed meat	g/capita^2/day	Shift
Dietary composition	Diets high in processed foods and additives	Diet high in sugar-sweetened beverages	g/capita^2/day	Shift
Dietary composition	Diets high in processed foods and additives	Diet high in sodium	g/capita^2/day	Shift

Dietary composition	Diets high in processed foods and additives	Diet high in trans fatty acids	% of energy intake /capita^2/day	Shift
Dietary composition	Diets high in animal whole foods	Diet high in red meat	g/capita^2/day	Shift
Dietary composition	Diets low in plant whole foods	Diet low in fruits	g/capita^2/day	Shift
Dietary composition	Diets low in plant whole foods	Diet low in vegetables	g/capita^2/day	Shift
Dietary composition	Diets low in plant whole foods	Diet low in whole grains	g/capita^2/day	Shift
Dietary composition	Diets low in plant whole foods	Diet low in legumes	g/capita^2/day	Shift
Dietary composition	Diets low in plant whole foods	Diet low in nuts and seeds	g/capita^2/day	Shift
Dietary composition	Diets low in essential nutrients and beneficial fatty acids	Diet low in calcium	g/capita^2/day	Shift
Dietary composition	Diets low in essential nutrients and beneficial fatty acids		% of energy intake /capita^2/day	Shift
Dietary composition	Diets low in essential nutrients and beneficial fatty acids		g/capita^2/day	Shift
Underweight		Low BMI	Diet low in polyunsaturated fatty acids	Scale
			Diet low in seafood omega-3 fatty acids	

The interaction between BMI and the 15 dietary risk categories is intended to control for confounders, such as body weight or physical activity, in the studies that provide relative risk estimates. However, the mediation between high BMI and dietary risks is minimal in the GBD studies, which typically exclude diets high in sugar-sweetened beverages when calculating the joint burden of dietary risks and high BMI.

The joint nature of the dietary risk exposures means that the output of attributable disease burden is provided as a total for the joint dietary risk exposure. A setting in the module can provide output in terms of attributions to individual exposure variables, but the results for individual components are given as attributable proportions of the YLLs and YLDs for joint exposure.

None of the disease outcomes from the BMI and weight-normalised dietary composition models involve protein-energy malnutrition. Therefore, the outputs of the simpler underweight model are considered additive and joint with the BMI and dietary composition output.

2.4.5 Formulas using a comparative risk methodology

The translation component of the dietary risk module outputs two sets of exposure parameters: mean exposure μ_{jasct} and standard deviation of exposure σ_{jasct} for risk factor $j \in J$ the subpopulation of country c in year t with age range a and sex s. Here J represent the set of risk factors in Table 4, which we can consider enumerated by

the row of Table 4 except the last row. Underweight and overweight use the same mean and standard deviation ($j = 1 = 15$) to parameterise an exposure distribution which is the distribution of BMI in the subpopulation - correspondingly the associated to. The dietary composition risks are associated to $j = 2, \dots, 14$, and the distributions of exposure parameterised by the mean and standard deviation are intake distributions (see Table 1). The disease rate projection components of the dietary risk module outputs the total incidence of diseases burdens in the subpopulations: YLL_{oasct} and YLD_{oasct} for the years of life lost to preventable mortality and morbidity, respectively, for disease outcome o (see Table 3) in country c in year t in individuals of with age range a and sex s.

To calculate the burden of disease from disease o attributed to a joint set J of dietary risk factors to in country c in individuals of age a and sex s, in year t,

$$YLL_{Joasct} = PAF_{Joasct,0}\left(\{\mu_{jasct}, \sigma_{jasct}\}_{j\in J}\right) \cdot YLL_{oasct} \quad (7)$$

and

$$YLD_{Joasct} = PAF_{Joasct,1}\left(\{\mu_{jasct}, \sigma_{jasct}\}_{j\in J}\right) \cdot YLD_{oasct} \quad (8)$$

where $PAF_{Joasct,0}$ and $PAF_{Joasct,1}$ are Population Attributable Fraction (PAF) for mortality and morbidity, respectively, for the joint set J of risk factors. These PAFS are called the joint PAFs, and they are derived from individuals PAFs.

To derive the Population Attributable Fraction (PAF) for disease o and outcome m (mortality $m = 0$ or morbidity $m = 1$) resulting from the risk factor $j \in J$ within a given country c, age group a and sex s in the year t, the exposure distributions are weighted by their relative risk factors and integrated against exposure x:

$$PAF_{joasct,m} = 1 - \frac{1}{\int_0^\infty RR_{joa,m}(x)\, P_{jasct}(\mu_{jasct}, \sigma_{jasct})(x)\, dx} \quad (9)$$

Here $P_{jasct}(\mu_{jasct}, \sigma_{jasct})$ is the probability distribution of exposure for risk factor j, parameterised by mean exposure μ_{jasct} and standard deviation of exposure σ_{jasct} provided by the translation component of the module. Here $RR_{joa,m}(x)$ is a relative risk function supported on the range $(0, \infty)$ that indicates an increased risk of disease outcome o and outcome m at age a if intake in category j is x units. For a diet low in consumption of a specific good, intake above the Theoretical Minimum Risk Exposure Level for adults ($TMREL_j$ – Table 1) is considered sufficient consumption and therefore assigned a relative risk factor value of 1. In analogy for any diet high in consumption, any value below $TMREL_j$ is given a relative risk factor of 1. If the subpopulation dietary intake probability distribution P_{jasct} is fully supported in the TMREL interval, then PAF_{joasct}=0. None of the disease outcomes are attributed to dietary intake. Up to a proportion of 1, PAF_{joasct} attributes the fraction of death and disability outcomes in disease o to dietary intake in the subpopulation *asc* at time *t* outside the TMREL interval.

The relative risk functions $RR_{joa,m}(x)$ are published in the form of a parameter $rf_{joa,m}$ and a unit parameter ν_j in the GBD study (Stanaway et al., 2018), (Afshin et al., 2019). The relative risk function has a different shape depending on whether risk increases with over (10) or underexposure (11):

$$RR_{joa,m}(x) = \begin{cases} rf_{joa,m}^{(x - TMREL_j)/\nu_j} & x \geq TMREL_j \\ 1 & 0 < x < TMREL_j \end{cases} \quad (10)$$

$$RR_{joa,m}(x) = \begin{cases} 1 & x \geq TMREL_j \\ {(TMREL_j - x)}/{\nu_j} & 0 < x < TMREL_j \\ rf_{joa,m} & \end{cases} \quad (11)$$

For risk of underweight or overweight, the TMREL is BMI=18.5 and BMI=30, respectively. Because underweight is calculated separately in the dietary risk module and added onto outputs from overweight and dietary composition at the end of the process, then for the purposes of these comparative risk formulas we can, without loss of generality, set $rf_{joa,m} = 1$ for $j = 15$. What this implies is that underweight attributed disease burden is zero from the comparative risk calculation, so there is no double counting with the separate calculation below for underweight. As described above, the parameters $rf_{joa,m}$ and $TMREL_j$ are internal to the GBD emulator component.

The PAFs for a given risk-disease pair in equation (9) are the fraction of total incidence of YLL or YLD associated with a given disease because of exposure, without considering incidence from other factors in the set the intake risk J. For summing up across different risk- disease pairs to get the joint PAF associated with joint exposure a mediation matrix is employed. The mediation factor MF_{jio} is the pairwise evaluation of a risk j mediated through exposure to factor i for disease o. To avoid double counting the attributed DALYs when risk factors share similar effects of exposure, the PAF for a joint set of risk factors $J \subset \{1, \dots, 15\}$ is derived according to Equation 12). The mediation factors are published for the 2017 study in the supplemental information of (Stanaway et al., 2018).

$$PAF_{Joasct,m} = 1 - \prod_{j=1}^{J} \left(1 - PAF_{joasct,m} \prod_{i=1}^{J} (1 - MF_{jio}) \right) \quad (12)$$

Once the GBD emulator component of the dietary risk module calculates equation (12), then it can combine with the output of the disease rate projection component and calculate (7) and (8).

Public health modelling following the methodology of the GBD attributes to a joint set of risk factors J the burden of disease o at the subpopulation a, s level in year t. This is the resolution of the public health modelling output. The total burden of disease in a country, across age groups, across genders, in a year or over time, or globally, due to the joint set of dietary risks J can be obtained by summing the values YLL_{Joasct} over the respective indices. For example, the burden of disease attributable to diets (all dietary risk factors in DALYs), in a subpopulation of country c at time t with age ranges $a \in A$ and sex s in year t is the sum of the burden of disease from all disease outcomes.

$$YLL_{JcAt} = \sum_{o,s,a \in A} PAF_{Joasct,0} \cdot YLL_{oasct} \quad (13)$$

$$YLD_{JcAt} = \sum_{o,s,a \in A} PAF_{Joasct,1} \cdot YLD_{oasct} \quad (14)$$

The outputs of attributable YLLs and YLDs for country c in year t in the age groups A and the risk factors J , when added to the underweight YLLs and YLDs below, is the output of the GBD emulator and the dietary risk module.

2.4.6 Limitations in using GBD emulators

For productivity losses from dietary risks, there are several limitations in the GBD models. Overlap between categories, such as sodium and processed meats or wholegrains and fibre, are imputed by simple mediation factors; moreover, relative risk factors and risk-outcome pairs change between studies (Beal et al. 2019; Stanton, 2024). The GBD uses historical consumption and outcomes in age groups from control studies as an indicator of

the burden of disease. To reflect the outcomes from consumption now, it assumes that the future dietary patterns and the preventative factors and technology remain similar to historical patterns. The GBD extrapolates dietary intake and its distribution in populations for national and sub-national population using statistical methods, and there can be significant differences in intake estimates between the GBD and other global sources such as the Global Dietary Database (GDD) (Beal et al.).

In Tables 1 and 4, the 13 dietary composition risk factors from the GBD model exclude diets low in milk and diets low in fibre to avoid double counting. The categories of diets low in milk and fibre are excluded because they are mediated in the GBD formulation of joint dietary risks with diets low in calcium and low in fruits, vegetables and wholegrains. Some nutrients and additives, like sodium, have a complicated relationship with processed meats and fruits and vegetable consumption, mediated by their effects on high systolic blood pressure. The modelling uses publicly available mediation factors used in the GBD model to take account into overlap between exposure and their effect on disease outcomes.

The dietary risk module uses a GBD 2017 emulator despite updates in 2019 and 2021 to the GBD models. Between the GBD 2019 and 2021 studies , the DALY estimates changed for most of the 13 composition categories, as the model updated its burden of proof, risk-outcome pairs and relative risk functions . Trans fat estimates, for example, for the same year were reduced by up to 90 percent in many countries, while disease burden from diets low in fruit increased. An error in the GBD 2017 and GBD 2019 trans-fat calculations were corrected in the GBD emulator. Disease burden from unprocessed red meat consumption experienced a sharp increase between the 2017 and 2019 rounds of the GBD study (Stanton, 2024), while, for example for Brazil, there was a reduction by nearly 50 percent between 2019 and 2021 (Lescinsky et al., 2022). In the GBD 2021 study, both diets low in milk and diets high in red meat intake have U-shaped relative risk curves (Lescinsky et al., 2022), meaning that both overconsumption of milk and underconsumption of red meat are associated with dietary risks, with this reflected in the modelling. Due to categorical quirks in the labelling of dietary risks in the GBD 2021, this sometimes results in a negative disease burden. For example, if the protective effect of consuming red meat outweighs its potential adverse health impacts, a diet high in red meat could be associated with a negative national disease burden in the GBD 2021 study. Overall, the relative risk factors for dietary risks are not stabilised, so the GBD 2017 model was preferred on these grounds and the fact that the representation of relative risk is more accessible in published supplemental information for the GBD 2017 version.

Underweight modelling is based on WHO's estimates of DALYs due to protein–energy malnutrition (Mathers, 2020). Protein–energy malnutrition is the only outcome considered. Nutrient deficiency and other disease outcomes from childhood malnutrition available from GBD models were not used. For adults, it is unclear how to resolve the potential double count between including additional nutrient deficiencies in hidden hunger, like calcium and iron deficiency, and the overlap between risk from diets low in fruits, vegetables, legumes, nuts and seeds, and diets high in red meat.

2.4.7 Formulas using a non-linear regression for underweight

The MAgPIE demand module outputs the prevalence ρ_{cAt} of adults underweight (BMI < 18.5) in country c in age group A in year t of frequency distribution. From exogenous economic and demographic projections GDP per capita in purchasing power parity (PPP) $GDPCAP_{ct}$ is given for country c in year t and the population POP_{cAt} in age group A. From this, denotes the fraction of population over the age of 65 (old-age dependency) $AGEDEP_{ct}$ is given for country c in year t. Let t_0 be the base year, for which it is assumed that the human development index HDI_{ct_0} of country c is known and the base year burdens of disease from protein-energy malnutrition YLL_{cAt_0} and YLD_{cAt_0} in country c in age group A are known. Historical data on years of life lost to mortality and morbidity per capita due to protein-energy malnutrition in an age group A across countries has quadratic form, which depends

linearly on the percentage of the population underweight and quadratically on HDI. Development can strongly prevent protein-energy YLLs and YLDs resulting from underweight individuals in the population. This relationship is denoted:

$$F_{A,m}(\rho, HDI) \tag{13}$$

where $\rho \in [0,1]$ is percentage of the population underweight and $HDI \in [0,1]$ is the human development index, and m represents mortality or morbidity outcomes. The human development index is used because it has greater predictive power than gross domestic product or gross income per capita. Generally, the historical relationship with mortality and morbidity from protein-energy malnutrition is not as strong for prevalence of underweight as for prevalence of undernourishment, (Lord, 2021). Fits for quadratic regression based on three coefficients average around adjusted $r^2 = 0.4$ across historical years and age groups.

Human development index (HDI) is not a direct output of MAgPIE or one of the macro-economic projections. However, HDI across countries has a very strong relationship to GDP PPP per capita and old age dependency, (Lord, 2023). This relationship, denoted

$$H(GDPCAP, AGEDEP) \tag{14}$$

where $GDPCAP \in [0, \infty)$ is percentage of the population underweight and $AGEDEP \in [0,1]$ is old age dependency (percentage of the national population over the age of 65). Where $\rho \in [0,1]$ is percentage of the population underweight and $HDI \in [0,1]$ is the human development index. Generally, the historical relationship is not as strong for prevalence of underweight as for prevalence of undernourishment. Fits using the four-parameter regression of the form average around adjusted $r^2 = 0.9$ across historical years.

$$(GDPCAP, AGEDEP) = 1 - exp\left(-a \cdot GDPCAP^{b} - c \cdot (AGEDEP \cdot GDPCAP)^{d}\right) \tag{15}$$

The approach used is to use the inputs from the MAgPIE demand module and economic and demographic projections to scale known years of life lost to mortality and morbidity in the modelling base year using historical relationships:

$$YLL_{cAt} = \frac{F_{A,0}\left(\rho_{cAt}, \frac{H(GDPCAP_{ct}, AGEDEP_{ct})}{H(GDPCAP_{ct_0}, AGEDEP_{ct_0})} \cdot HDI_{ct_0}\right)}{F_{A,0}\left(\rho_{cAt_o}, HDI_{ct_0}\right)} \cdot \frac{POP_{cAt}}{POP_{cAt_0}} \cdot YLL_{cAt_0} \tag{16}$$

$$YLD_{cAt} = \frac{F_{A,1}\left(\rho_{cAt}, \frac{H(GDPCAP_{ct}, AGEDEP_{ct})}{H(GDPCAP_{ct_0}, AGEDEP_{ct_0})} \cdot HDI_{ct_0}\right)}{F_{A,1}\left(\rho_{cAt_o}, HDI_{ct_0}\right)} \cdot \frac{POP_{cAt}}{POP_{cAt_0}} \cdot YLD_{cAt_0} \tag{17}$$

Bayesian quadratic regression can be used to introduce uncertainty in the regression form based on the empirical data.

2.5 Output

Intended output is joint YLL and YLD attributable to the exposure to dietary risks determined from the MAgPIE demand module and exogenous economic and demographic projections. Output is provided per country in three age brackets (15-44, 45-69, 70+). Currently, estimates are not provided for children (0-15 years). The age brackets allow better resolution for disease burden in working age groups and potential productivity losses.

A flag provided to the dietary risk module allows optional output of attributable fractions of the joint disease burden among the individual dietary risk factors in Table 1 also by country and age bracket.

Through the GBD emulator and the Bayesian regression for underweight the models in the dietary risk module have the capacity to generate output that accounts for uncertainty in the disease burden projections. The ability to use the uncertainty features in the models with a hard coupling with MAgPIE are still being evaluated due to the challenges of runtime, storage of Monte-Carlo runs, and conforming with MAgPIE specifications.

2.6 Further enhancements done in MAgPIE

The primary focus of enhancements to MAgPIE under DIAMOND shifted toward developing a health module to evaluate public health co-benefits of land-use and dietary transitions. However, several additional model improvements and contributions are pursued beyond this health-focused enhancement. These include the development of an emulator to support joint biodiversity and climate scenario analysis, incorporation of a refined costing framework aligned with spatial land-use strategies, and the integration of Nature-based Solutions (NbS) into land allocation and mitigation assessments. While the originally proposed updates to agricultural economic parameters were made redundant by upstream improvements in the core model, the work under Task 4.2 significantly broadened MAgPIE's capabilities to interface with energy system models, evaluate biodiversity outcomes, and assess NbS in transition pathways. These are outlined in the following subsections.

2.6.1 Work in support of joint climate and biodiversity scenarios

To assess biodiversity outcomes under stringent climate mitigation scenarios, Oxford University in cooperation with other institutes is developing an emulator of the MAgPIE land-use model, designed to interact with the energy systems models. The emulator enables efficient representation of complex land-use dynamics within broader integrated assessment modelling. It is built from a scenario matrix generated by systematically varying bioenergy and carbon price trajectories in MAgPIE, under different levels of biodiversity protection ambition. Each scenario captures key land-system indicators, such as bioenergy production potentials, AFOLU (agriculture, forestry and other land use) emissions, land-use change, and the Biodiversity Intactness Index (BII). These scenario outputs are structured into a lookup table format, which can then be ingested by IAMs. During optimisation, an IAM can linearly combine scenarios from this matrix to meet its energy system demands for bioenergy, while also internalising associated land-use impacts and emissions. To ensure that land-use change emissions are not underestimated, the emulator incorporates enhancements that account for the historical emissions trajectory required to reach a given virtual scenario. This coupled system enables the exploration of synergistic or conflicting outcomes of biodiversity restoration and climate mitigation, allowing for robust policy assessment under PARIS-aligned carbon budgets.

Considering that topics related to biodiversity emerged as a key theme in the multi-stakeholder discussion groups, this work will be relevant for the DIAMOND project for setting appropriate initial conditions for the DIAMOND IAMs (crucially including OMNIA and OPEN-PROM; see Sections 3 and 4) ensuring convergence of joint optimisation between MAgPIE and the IAMs.

2.6.2 Cost Modelling in DIAMOND

The latest version of the MAgPIE model includes improved cost assumptions as originally proposed in Vittis et al. (2021). These were implemented and integrated in full in Vittis et al. (2024), fulfilling the earlier commitment to enhance the model's costing module. As this update was carried out by the core MAgPIE team, additional work on further refining the costing structure is currently considered redundant. Moreover, any further updates would require substantial recalibration efforts and are therefore not planned in the near future. However, the MAgPIE

version used in DIAMOND—including updates and links to IAMs as described in Section 3—ensured the incorporation of the updated costing assumptions (Vittis et al. 2024), ensuring consistency with the updated performed in the IAMs.

2.6.3 Representation of Nature-based Solutions in MAgPIE

In MAgPIE, Nature-based Solutions (NbS) are modelled through explicit conservation and restoration strategies embedded in both the land-use optimisation and spatial allocation modules. MAgPIE integrates NbS through imposing area-based constraints, such as those related to protected areas and restoration targets, to restrict agricultural expansion and promote regrowth of forests or semi-natural land, while accounting for their opportunity costs in terms of foregone yields and additional land-use investments. During scenario simulations, alternative NbS-rich pathways (e.g., 'PROTECT', 'COACTION', 'MULTI') impose quantitative targets, such as conserving ≥ 20% of semi-natural habitat in agricultural landscapes, to maintain biodiversity, enhance pollination sufficiency, and reduce soil erosion. These constraints are spatially resolved, using high-resolution ecological data from the SEALS downscaling framework, ensuring that restoration and protection are targeted in ecologically meaningful locations. The model incorporates carbon stock recovery from land set aside as negative emissions and factors in the economic trade-offs via heightened land-use costs and moderated yield intensification.

These functionalities significantly improve policy analysis by enabling the exploration of integrated strategies that jointly address climate, biodiversity, and land-use objectives. Policymakers can now evaluate the implications of biodiversity protection targets, e.g., "30x30" or biome-specific BII thresholds, under varying carbon budgets and bioenergy deployment levels. In doing so, MAgPIE supports the identification of land-based mitigation portfolios that avoid unintended ecological damage, such as the conversion of biodiverse landscapes for biomass production to generate net-negative carbon emissions through the deployment of CCS on modern biomass power plants and biorefineries; over-reliance on negative emissions technologies such as BECCS has been a longstanding criticism of IAMs (Gambhir et al., 2019). The endogenous treatment of agricultural intensification also allows quantifying the costs and limits of land-sparing approaches, providing key insights into how much yield growth is needed to achieve NbS targets without expanding cropland or pasture.

The enriched representation of NbS enables new lines of inquiry: What trade-offs emerge when negative emissions targets compete with biodiversity protection? How much land can feasibly be set aside or restored without jeopardising food security? What regions offer the most cost-effective opportunities for biodiversity-friendly mitigation? These questions are especially relevant in the context of aligning nationally determined contributions (NDCs) with the Kunming-Montreal Global Biodiversity Framework and evolving EU restoration legislation. DIAMOND aims to scope the alignment of these capabilities with the research questions elicited through the stakeholder engagement activities to inform the scenarios analysed in WP5.

Nonetheless, the model has limitations for decision-making at finer scales. MAgPIE is not designed to represent land-sharing approaches, where biodiversity is integrated within productive landscapes through agroecology or mixed-use farming. Instead, NbS are implemented via a land-sparing logic, wherein conservation and restoration occur primarily on marginal or reallocated land made available through productivity gains. Furthermore, biodiversity is measured primarily through the Biodiversity Intactness Index (BII), a spatially aggregated indicator that does not capture habitat quality, species richness, or the needs of conservation at the local scale. The BII also does not account for connectedness of landscape structures that are conducive to biodiversity enrichment. Consequently, while MAgPIE offers strategic insights for global and regional policy design, its outputs should be complemented with place-based ecological assessments and stakeholder-informed planning tools when applied to national or subnational decision-making contexts. Finally, MAgPIE is used to assess broad policies and typically is not used for the assessment of concrete implementation policies on the level of detailed policy instruments.

3 Soft-Linking & Integration of Omnia and MAgPIE

There are many land-related uncertainties related to delivering net zero targets at the regional and global level. In particular, overreliance on the natural land sink to compensate for emissions in hard-to-abate sectors could prove risky, given the large uncertainties in the response of terrestrial carbon sinks to environmental drivers. Such challenges require a better linkage between energy system models, in our case OMNIA, and the land use model MAgPIE to better understand land uncertainties in low carbon transition pathways.

Furthermore, quantifying the interconnection between land, energy and food is critical. To achieve net-zero emissions and the Sustainable Development Goals (SDGs), we need to identify solutions that balance these multiple objectives. There are many trade-offs to consider; for example, expanding biomass-based energy fuels may reduce our dependence on fossil fuels and lower emissions in one sector, but it can also lead to deforestation, a decrease in land sinks, loss of biodiversity, and food insecurity. Understanding these model linkages will help us assess such trade-offs, quantify interconnections, and identify "no regrets strategies".

Based on these identified research needs, soft-linking MAgPIE and OMNIA is needed to achieve the following objectives:

- Improve the representation of Agriculture, Forestry and Other Land Uses (AFOLU) emissions in OMNIA,
- Provide more accurate bioenergy production and related costs and GHG emissions in OMNIA.

In the following we describe the soft-link between the two models (Section 3.1) and provide preliminary results that highlight the functionalities of the integrated system (Section 3.2).

3.1 Introduction to MAgPIE and the need to link to OMNIA

The soft-link between OMNIA and MAgPIE focuses on two critical interactions (see Figure 2) related to:

- Bioenergy demand and supply,
- Land Use and Land Use Change GHG emissions and GHG prices.

OMNIA provides MAgPIE with the level of biomass and bioenergy demand and CO_2 prices under different scenarios of socio-economic and global temperature evolution, while MAgPIE provides biomass costs associated with the biomass supply (to meet the biomass demand calculated by OMNIA) and related land use GHG emissions when producing the requested amount of bioenergy under the same socio-economic and global temperature scenarios.

Funded by
the European Union

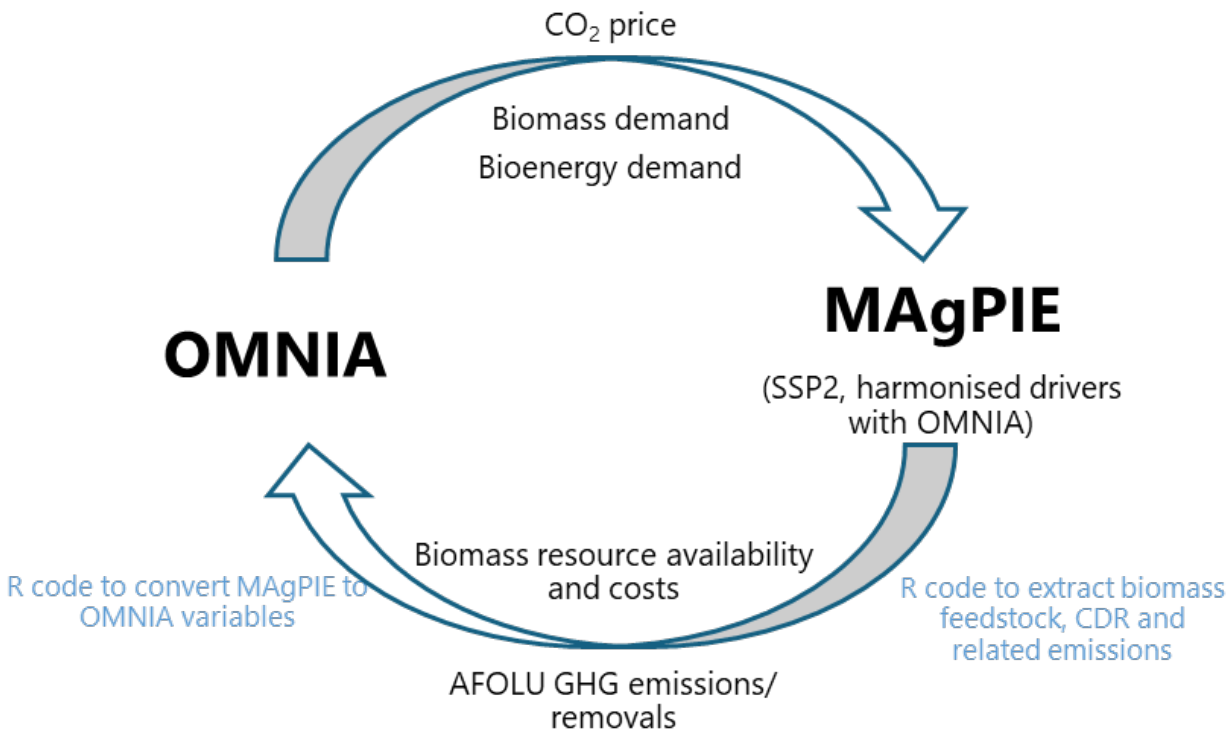

Figure 2. Soft-linking between OMNIA and MAgPIE. OMNIA provides MAgPIE with the level of biomass and bioenergy demand and CO_2 prices, while MAgPIE provides costs and related GHG emissions when producing the requested amount of bioenergy under the same socio-economic scenarios.

3.1.1 Customising MAgPIE to be compatible with OMNIA

Using the original configuration of MAgPIE, biomass production and related land use and land use change emissions can be plotted for the default 12 global regions, which do not match the 28 regions in OMNIA. Furthermore, to integrate MAgPIE results into OMNIA, future land-use in MAgPIE needs to be harmonised with the OMNIA socio-economic settings, represented by the Shared Socioeconomic Pathways (SSPs) narratives and model implementation. In the following subsections, we explain how we mapped OMNIA regions in MAgPIE and harmonised future socio-economic assumptions (SSPs) between the two models.

3.1.2 Regional detail

There are two ways to approach the harmonisation of regional disaggregation between the two models:

1. Run MAgPIE using the original configuration of 12 regions, and then disaggregate the results to fit the 28 regions of the OMNIA model; or
2. Recalibrate the clusters in the LPJML model based on the OMNIA regions and then run the MAgPIE model with the OMNIA regional configuration.

For the soft linking in this project, we selected the second approach. This implies considering the biophysical variables on the most disaggregated MAgPIE resolution, i.e., 200 clusters, each one being a spatial aggregate of 05x05 grid cells with similar properties (Dietrich et al., 2019). Then we grouped these clusters into the 27 regions of OMNIA (see Table 6 and Figure 3) and run the optimisation problem on the aggregated 27 regions. We note that the inclusion of more clusters in a region consequently lead to a higher biophysical detail within the region. Due to the small size of Japan and South Korea, these three regions were combined in MAgPIE, although separated in OMNIA.

Funded by the European Union

Table 6. Geographical representation on OMNIA regions in MAgPIE including the number of original clusters in each region.

Region name	East Africa	North Africa	West Africa	Southern Africa	Australia and New Zealand	Central Asia	South-East Asia	South Asia	Brazil
Acronym	AFE	AFN	AFW	AFZ	ANZ	ASC	ASE	ASO	BRA
Clusters	8	12	15	11	10	9	5	7	5
Region name	Canada	Chile	China	non-EU Eastern Europe	non-EU Western Europe	Eastern EU	Mediterranean EU	non-EU Western EU	Indonesia, Philipine, Vietnam
Acronym	CAN	CHL	CHN	ENE	ENW	EUE	EUM	EUW	IDN
Clusters	5	5	17	2	3	2	6	7	6
Region name	India	Japan+S. Korea	Latin America	Mediterranean Asia	Middle East	Mexico	Nigeria	Russia	United States
Acronym	IND	JSK	LAM	MDA	MEA	MEX	NIG	RUS	USA
Clusters	4	4	12	3	7	5	4	14	12

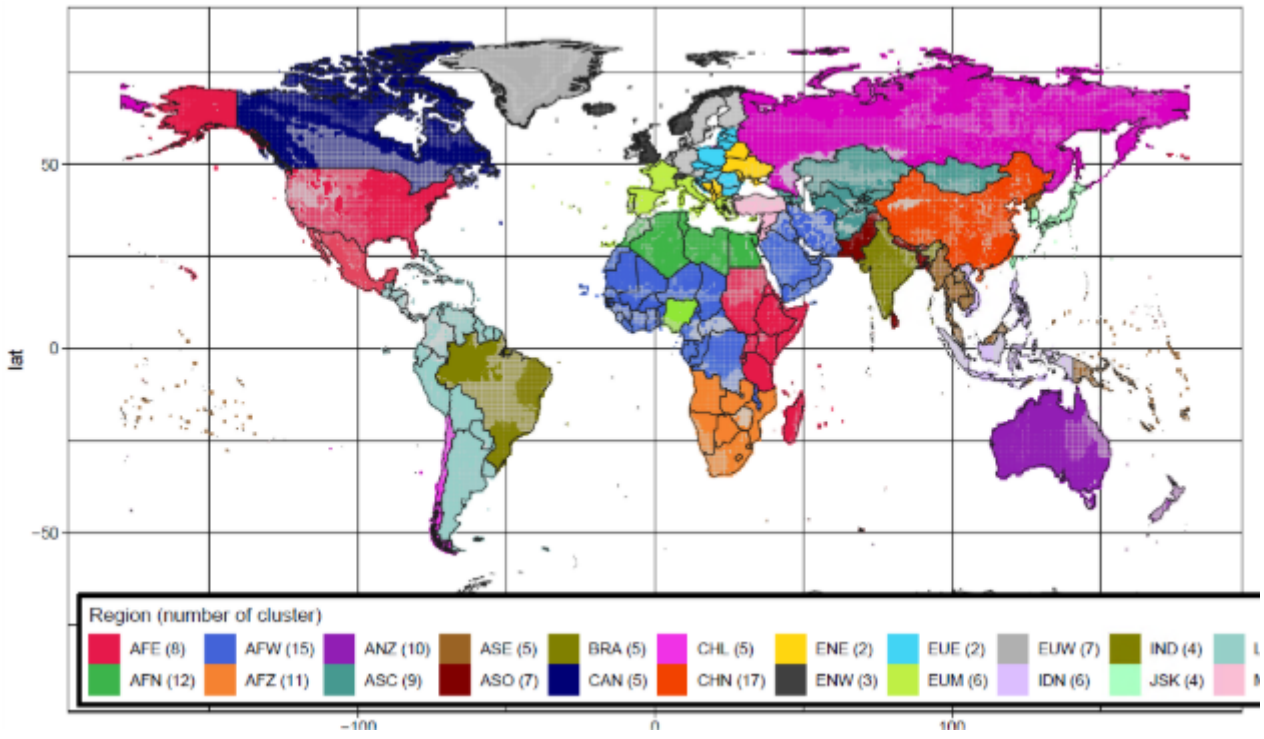

Figure 3. Visual graph for the geographical representation on OMNIA regions in MAgPIE including the number of original clusters in each region.

3.1.3 Socio-economic settings

MAgPIE v. 4.8.2 (Dietrich et al., 2024) utilised in this work runs on the older definitions of SSPs (Riahi et al., 2017). Work has been done to update the population and GDP assumptions, which act as main drivers in both models, to match the latest sets of SSPs utilised in the OMNIA runs (SSP v. 3.1.0). The suggested harmonisation catalogue

outlined in D3.2 was followed to ensure consistency between the two models, and developments in the other models of DIAMOND. A patch for updating national policies and Nationally Determined Contributions (NDCs) has been also created to update these policies in this version of MAgPIE, to match the OMNIA settings. This has been done for all SSPs (SSP1, 2, 3 4 and 5), but for the first soft-link between MAgPIE and OMNIA only SSP2 was used.

3.1.4 Mapping MAgPIE outputs to OMNIA inputs

Biomass and bioenergy are used in different parts of the energy sector, as represented in Figure 4. Biomass as feedstock (primary energy) is composed of energy crops (crops purposely cultivated for energy), food crops (which provide 1st generation biofuels, e.g., ethanol), and solid biomass (encompassing traditional biomass, agricultural and forest residues). Biomass feedstock is then converted to different forms of energy, which are then utilised in diverse end-use sectors (buildings, transport and industries) and in the power sector in OMNIA.

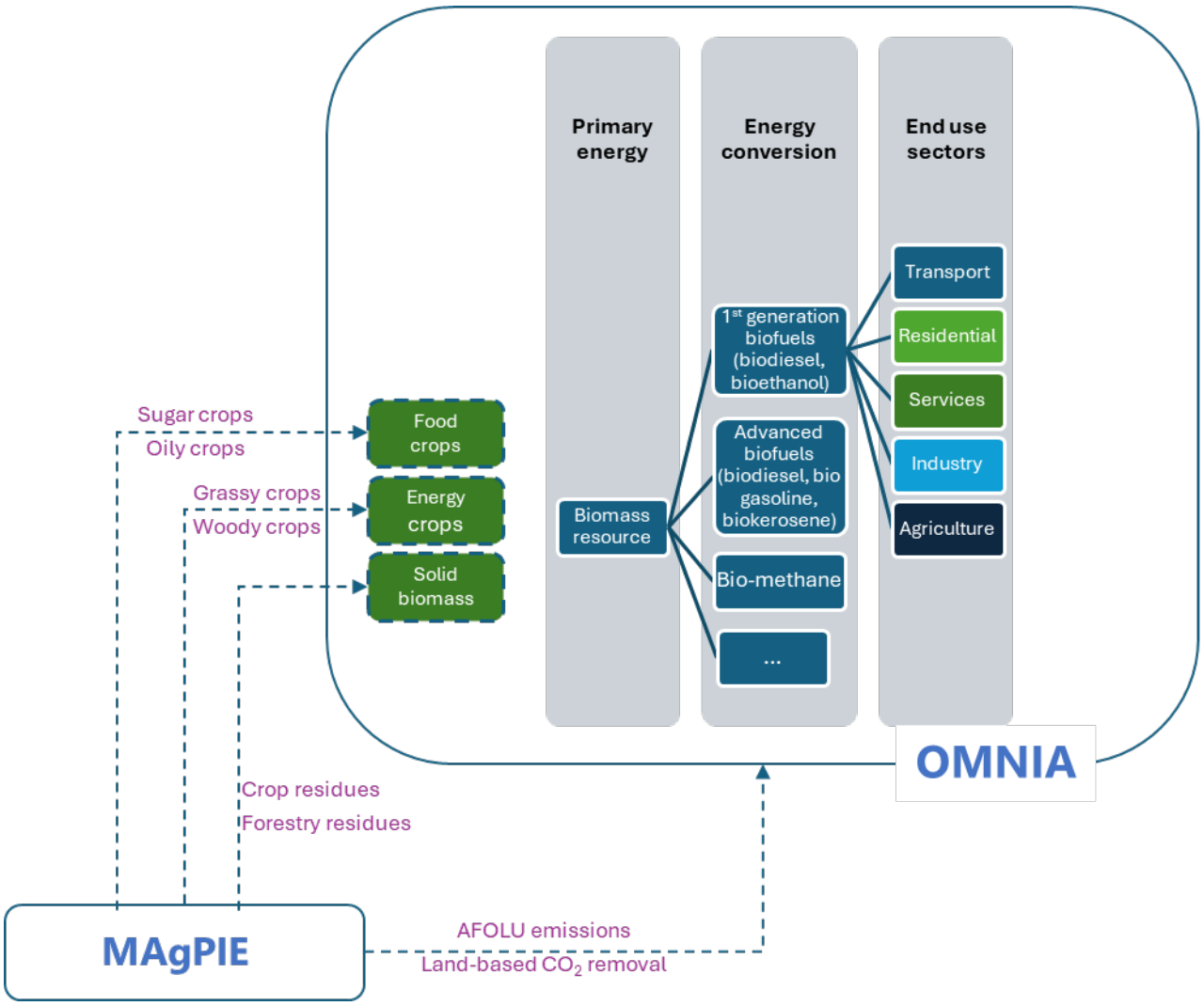

Figure 4. High-level representation of biomass and bioenergy in OMNIA and MAgPIE.

At a more disaggregated level, MAgPIE provides OMNIA with detailed information on individual biomass types and their associated prices, enabling the differentiated representation shown in Figure 5 below.

The data collected from MAgPIE on all variables of interest includes amount (EJ/yr), cost (US$2017/EJ), and emissions (Mt CO2/yr). Note that the emissions are provided per sector overall, i.e., land-use or agriculture, rather than per individual crop.

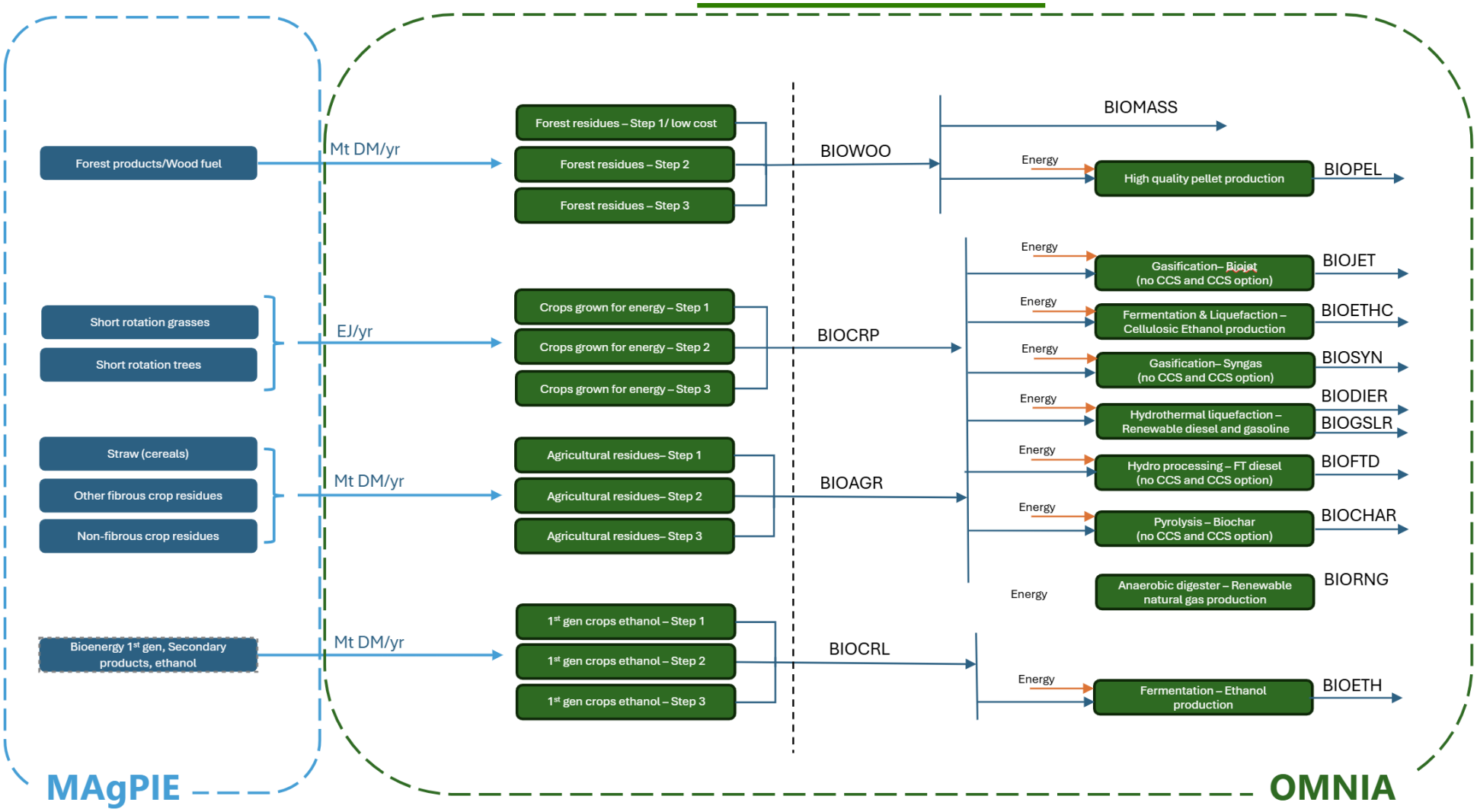

Figure 5. Detailed representation of the MAgPIE to OMNIA mapping, including the different types of biomass and bioenergy and associated costs. For instance, 'agricultural residues' in OMNIA come from three different types of crop residues in MAgPIE, i.e. cereal straw, rice husks (fibrous residues) and other crop residues (non-fibrous residues).

Funded by the European Union

3.1.5 Procedure for MAgPIE data extraction for OMNIA

An additional tailored script has been written in the R language to extract variable outputs from MAgPIE rds format to csv format required in OMNIA. These variables are extracted in the IAMC data format, to enable comparability and readability across all models updated in DIAMOND. Figure 6 below showcases selected MAgPIE variables extracted over the whole modelling horizon, from present time to 2100.

```
# Assuming 'df' is your DataFrame
selected_value = "Production|+|Crop residues"
selected_value = "Production|Forest products|+|Wood fuel"
selected_value = "Production|Secondary products|+|Ethanol"
selected_value = "Production|Bioenergy|2nd generation|++|Bioenergy crops"
```

Figure 6. Biomass feedstock and biofuel data extraction from MAgPIE for OMNIA use.

Note that for all variables, MAgPIE was run at different biomass feedstock costs to extract the data necessary for the supply cost curves to be used by OMNIA. The final data tables prepared for OMNIA are formatted to OMNIA requirements as in the example presented in Figure 6, illustrating the availability of energy crops over the time horizon.

3.2 Preliminary results

As an illustration of the process for the extraction of results, in the following section we show the availability of different biomass types per OMNIA region. Figure 7 shows MAgPIE 2nd generation crop availability per region and cost range which acts input to OMNIA; Figure 8 presents the total regional available bioenergy; Figure 9 the availability of energy crops (only the 2nd generation bioenergy); and Figure 10 crop residues for energy uses, mainly comprised by straw.

Funded by
the European Union

variable	cost	year	0	1	2	3	4	5	6	7	8	9	10	11	12	13	14	15	16	17	18	19	20	21	22	23	24	25	26	27
EJ/yr	$/t	region	AFE	AFN	AFW	AFZ	ANZ	ASC	ASE	ASO	BRA	CAN	CHL	CHN	ENE	ENW	EUE	EUM	EUW	IDN	IND	JPN	SKO	LAM	MDA	MEA	MEX	NIG	RUS	USA
2nd gen energy crops	5	1995	0	0	0	0	0	0	0	0	0	0	0	0	0	0	0	0	0	0	0	0	0	0	0	0	0	0	0	0
2nd gen energy crops	5	2000	0	0	0	0	0	0	0	0	0	0	0	0	0	0	0	0	0	0	0	0	0	0	0	0	0	0	0	0
2nd gen energy crops	5	2005	0	0	0	0	0	0	0	0	0	0	0	0	0	0	0	0	0	0	0	0	0	0	0	0	0	0	0	0
2nd gen energy crops	5	2010	0	0	0	0	0	0	0	0	0	0	0	0	0	0	0	0	0	0	0	0	0	0	0	0	0	0	0	0
2nd gen energy crops	5	2015	0	0	0	0	0	0	0	0	0	0	0	0	0	0	0	0	0	0	0	0	0	0	0	0	0	0	0	0
2nd gen energy crops	5	2020	0	0	0	0	0	0	0	0	0	0	0	0	0	0	0	0	0	0	0	0	0	0	0	0	0	0	0	0
2nd gen energy crops	5	2025	0	0	0	0	0	0	0	0	0	0	0	0	0	0	0	0	0	0	0	0	0	0	0	0	0	0	0	0
2nd gen energy crops	5	2030	0	0	0	0	0	0	0	0	0	0	0	0	0	0	0	0	0	0	0	0	0	0	0	0	0	0	0	0
2nd gen energy crops	5	2035	0	0	0	0	0	0	0	0	0	0	0	0	0	0	0	0	0	0	0	0	0	0	0	0	0	0	0	0
2nd gen energy crops	5	2040	0	0	0	0	0	0	0	0	0	0	0	1	0	0	0	0	0	0	0	0	0	0	0	0	0	0	0	0
2nd gen energy crops	5	2045	0	0	0	0	0	0	0	0	0	0	0	1	0	0	0	0	0	0	0	0	0	0	0	0	0	0	0	1
2nd gen energy crops	5	2050	0	0	0	0	0	0	0	0	1	0	0	3	0	0	0	0	0	0	0	0	0	1	0	0	0	0	0	1
2nd gen energy crops	5	2055	1	0	1	0	0	0	0	1	1	0	0	5	0	0	0	0	0	1	0	0	0	1	0	0	1	0	0	3
2nd gen energy crops	5	2060	2	0	2	1	0	0	1	1	2	0	0	7	0	0	0	0	0	1	0	0	0	2	0	0	1	1	0	5
2nd gen energy crops	5	2070	4	0	4	2	0	0	2	3	3	0	0	10	0	0	1	1	1	3	0	1	1	4	0	0	2	2	0	8
2nd gen energy crops	5	2080	5	0	5	3	0	0	3	5	4	0	0	11	0	0	0	1	1	5	0	1	1	5	0	0	2	3	0	10
2nd gen energy crops	5	2090	8	0	8	4	0	1	4	7	4	0	0	9	0	0	0	1	0	7	0	1	1	6	0	0	2	4	1	11
2nd gen energy crops	5	2100	10	0	10	5	0	1	4	8	12	0	0	20	1	0	0	0	0	8	1	1	1	8	1	0	2	6	1	10
2nd gen energy crops	10	1995	-	-	-	-	-	-	-	-	-	-	-	-	-	-	-	-	-	-	-	-	-	-	-	-	-	-	-	-
2nd gen energy crops	10	2000	-	-	-	-	-	-	-	-	-	-	-	-	-	-	-	-	-	-	-	-	-	-	-	-	-	-	-	-
2nd gen energy crops	10	2005	-	-	-	-	-	-	-	-	-	-	-	-	-	-	-	-	-	-	-	-	-	-	-	-	-	-	-	-
2nd gen energy crops	10	2010	-	-	-	-	-	-	-	-	-	-	-	-	-	-	-	-	-	-	-	-	-	-	-	-	-	-	-	-
2nd gen energy crops	10	2015	-	-	-	-	-	-	-	-	-	-	-	-	-	-	-	-	-	-	-	-	-	-	-	-	-	-	-	-
2nd gen energy crops	10	2020	-	-	-	-	-	-	-	-	-	-	-	-	-	-	-	-	-	-	-	-	-	-	-	-	-	-	-	-
2nd gen energy crops	10	2025	-	-	-	-	-	-	-	-	-	-	-	-	-	-	-	-	-	-	-	-	-	-	-	-	-	-	-	-
2nd gen energy crops	10	2030	-	-	-	-	-	-	-	-	-	-	-	-	-	-	-	-	-	-	-	-	-	-	-	-	-	-	-	-
2nd gen energy crops	10	2035	-	-	-	-	-	-	-	- 0	-	-	-	-	-	-	-	-	-	-	-	-	-	0	-	-	-	-	-	-
2nd gen energy crops	10	2040	-	0	-	-	-	-	- 0	- 0	-	-	-	-	-	-	-	-	-	-	-	-	-	0	-	-	- 0	-	-	-
2nd gen energy crops	10	2045	-	-	-	-	-	-	- 0	- 0	-	-	-	-	-	-	-	- 0	-	-	- 0	0	0	-	-	0	-	-	-	0
2nd gen energy crops	10	2050	-	-	-	-	- 0	-	- 0	-	-	-	-	-	-	-	-	- 0	-	-	- 0	0	0	- 0	-	0	-	-	-	-
2nd gen energy crops	10	2055	-	-	-	-	-	-	- 0	-	-	-	-	-	-	-	-	- 0	-	-	- 0	0	0	-	- 0	-	0	-	-	-
2nd gen energy crops	10	2060	-	-	-	-	-	-	- 0	-	-	-	-	-	-	-	-	- 0	-	-	- 0	0	0	- 0	0	-	-	0	-	- 0
2nd gen energy crops	10	2070	-	-	-	-	-	-	- 0	-	-	-	-	-	-	-	-	- 0	-	-	- 0	0	0	- 0	-	-	-	-	0	- 0
2nd gen energy crops	10	2080	-	-	-	0	-	-	0	- 0	17	-	-	0	-	0	-	- 0	-	-	- 0	0	0	7	-	-	-	-	2	- 0
2nd gen energy crops	10	2090	7	-	48	15	4	-	31	-	43	11	-	25	2	1	0	1	-	32	- 0	0	0	97	-	-	5	-	2	24
2nd gen energy crops	10	2100	8	-	42	30	27	-	58	-	55	19	0	59	5	1	1	7	0	43	21	1	1	165	0	-	11	1	5	72
2nd gen energy crops	15	1995	-	-	-	-	-	-	-	-	-	-	-	-	-	-	-	-	-	-	-	-	-	-	-	-	-	-	-	-
2nd gen energy crops	15	2000	-	-	-	-	-	-	-	-	-	-	-	-	-	-	-	-	-	-	-	-	-	-	-	-	-	-	-	-
2nd gen energy crops	15	2005	-	-	-	-	-	-	-	-	-	-	-	-	-	-	-	-	-	-	-	-	-	-	-	-	-	-	-	-
2nd gen energy crops	15	2010	-	-	-	-	-	-	-	-	-	-	-	-	-	-	-	-	-	-	-	-	-	-	-	-	-	-	-	-
2nd gen energy crops	15	2015	-	-	-	-	-	-	-	-	-	-	-	-	-	-	-	-	-	-	-	-	-	-	-	-	-	-	-	-
2nd gen energy crops	15	2020	-	-	-	-	-	-	-	-	-	-	-	-	-	-	-	-	-	-	-	-	-	-	-	-	-	-	-	-
2nd gen energy crops	15	2025	-	-	-	-	-	-	-	-	-	-	-	-	-	-	-	-	-	-	-	-	-	-	-	-	-	-	-	-
2nd gen energy crops	15	2030	-	-	-	-	-	-	-	-	-	-	-	-	-	-	-	-	-	-	-	-	-	-	-	-	-	-	-	-
2nd gen energy crops	15	2035	-	-	-	-	-	-	0	-	-	-	-	-	-	-	-	-	-	-	-	-	-	-	-	-	-	-	-	-
2nd gen energy crops	15	2040	-	-	-	- 0	-	-	0	0	-	-	-	-	-	-	0	-	-	- 0	- 0	-	-	-	-	-	0	-	-	-
2nd gen energy crops	15	2045	-	-	-	-	-	-	0	0	-	-	-	-	-	-	-	0	-	- 0	0	- 0	- 0	-	-	- 0	-	-	-	- 0
2nd gen energy crops	15	2050	-	-	-	-	0	-	0	- 0	-	-	-	-	-	-	-	0	-	-	- 0	- 0	- 0	0	-	-	- 0	-	-	-
2nd gen energy crops	15	2055	-	-	-	-	-	-	0	- 0	-	-	-	-	-	-	-	0	-	-	- 0	- 0	- 0	0	- 0	-	-	-	-	-
2nd gen energy crops	15	2060	-	-	-	-	-	-	0	- 0	2	0	-	-	-	-	-	0	-	-	- 0	- 0	- 0	0	- 0	-	-	-	1	0
2nd gen energy crops	15	2070	-	- 0	12	1	-	-	19	- 0	35	-	-	-	0	-	0	0	-	23	- 0	0	0	38	-	-	-	-	2	0
2nd gen energy crops	15	2080	7	-	52	16	4	-	42	0	24	10	0	3	2	0	2	3	-	31	1	0	0	63	-	-	3	-	0	23
2nd gen energy crops	15	2090	3	0	2	10	23	0	15	-	8	5	2	36	3	0	3	3	-	1	15	1	1	34	-	-	4	-	18	8
2nd gen energy crops	15	2100	16	-	31	0	16	4	- 1	-	1	2	4	6	2	2	6	- 2	2	- 0	4	0	0	6	1	3	1	- 1	22	5

Figure 7. MAgPIE energy crop availability at different prices in each region, over the modelling time, exported from MAgPIE to OMNIA, in OMNIA format for SSP2 analysis.

A better view of the cost-supply curves presented in Figure 7 is represented in Figure 8, showing bioenergy production over time (2020 to 2100) in each region. Interestingly, 2nd generation bioenergy (green shades) completely overtakes 1st generation bioenergy (red shade, made up of both 1st gen biodiesel and bioethanol) across all regions. This is due to the assumption in MAgPIE that 1st generation biofuels are slowly being phased out by the more efficient 2nd generation biofuels, also reducing competition for land with food and other human uses (Bauer et al., 2020).



Figure 8. Total bioenergy production, with 2nd generation bioenergy in green shade and 1st generation bioenergy in red shade

Going into further detail of the type of energy crop cultivated, Figure 9 shows the production of different types of crops cultivated by region over time, grouped under two key types of crops: grasses (green shade) and trees (red trees). We note that there is a strong adoption of grasses, i.e., miscanthus, across all regions except for non-EU Western Europe (ENW), where tree crops are predominating, especially after 2050. This behaviour is explained by how MAgPIE calculates demand for bioenergy, i.e., by minimising the cost of agricultural production (solved in 10-year time steps until 2095 in recursive dynamic mode) by varying the spatial production patterns through expanding crop land and by investing in yield-increasing technology changes (Dietrich et al 2014, Lotze- Campen et al 2014). Technology change increases the potential yields of all crops within a region by the same factor. The costs for enhancing the yields in a specific region increase with the level of agricultural development of that region, i.e., the higher the actual yields in a region, the higher the costs for one additional unit of yield increase (Dietrich et al 2014).

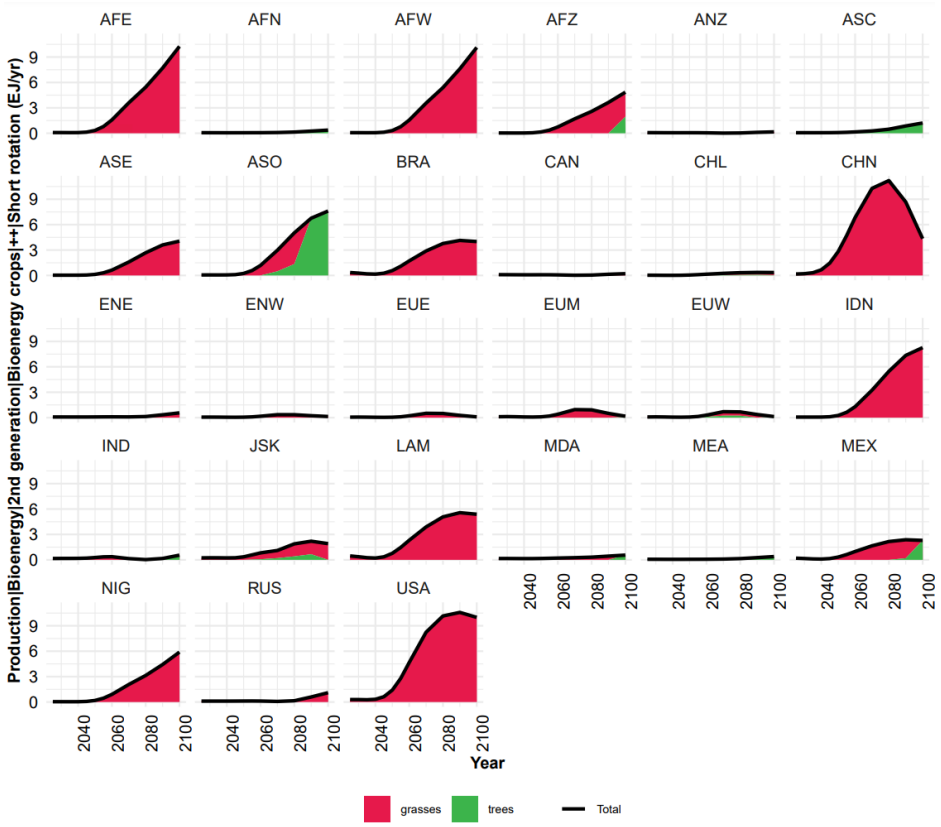

Figure 9. Regional energy crop production by biomass type, green shade denoting trees, red shade denoting grasses

In parallel with new crop production, to meet high bioenergy demand, MAgPIE also utilises three types of crops residues, see Figure 10, with blue shade denoting straw (cereal residues), green shade denoting other fibrous crop residues (e.g. rice husks), and red denoting non fibrous crop residues (e.g. corn stove). It is interesting to note that except for Russia, straw completely dominates the residues generation across all regions. Note that residue production is driven by food crop production, not by a carbon price. Furthermore, crop residues can be burned, used for feed, recycled to soils or used for other purposes (construction, fuel, etc.). The amount of residues available for energy uses is calculated in MAgPIE after extracting the fraction of residues needed to remain onsite to ensure long term nutrient circulation (Dietrich et al., 2024).

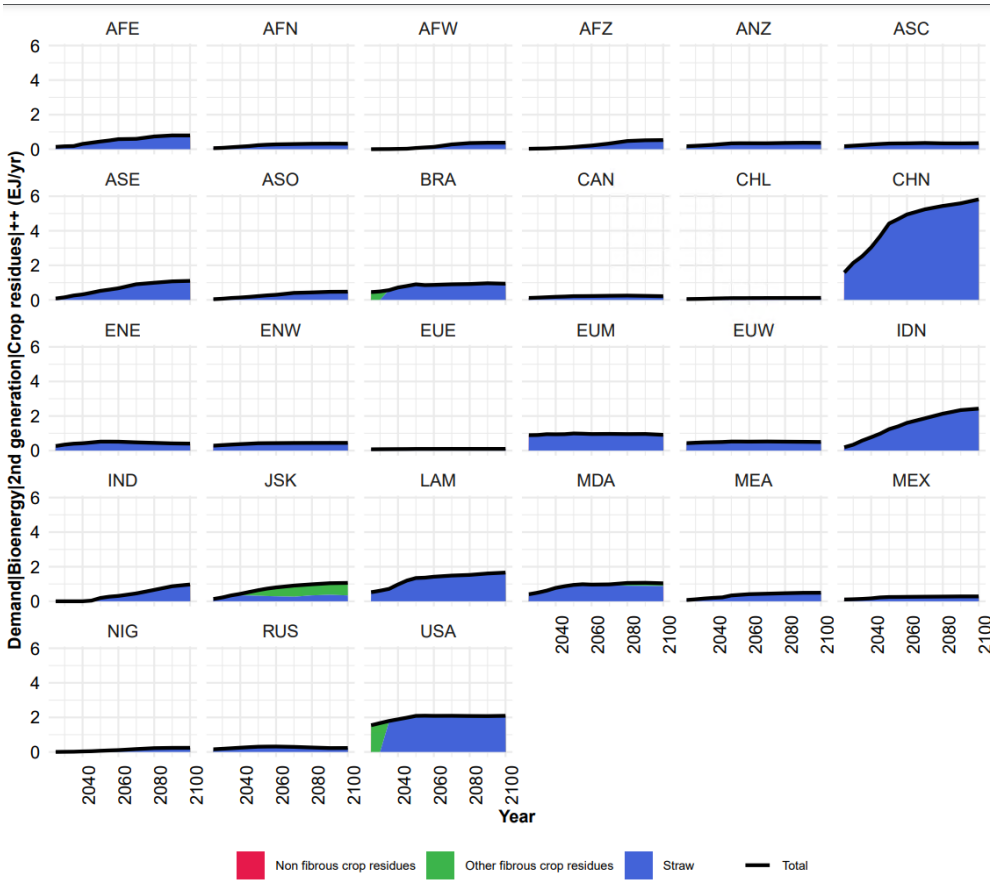

Figure 10. Regional crop residues available for energy production by type, blue shade denoting straw (cereal residues), green shade denoting other fibrous crop residues (e.g. rice husks), and red denoting non fibrous crop residues (e.g. corn stove)

The important 2nd generation bioenergy production expansion under SSP2 futures under NDC policies comes at the expense of intense land use change, in particular in Brazil (up to 30 million ha conversion by 2100), China (up to 35 million ha conversion by 2070, then reducing afterwards), and USA (25 million ha by 2060), see Figure 11.



Figure 11. Regional land expansion of 2nd generation energy crops (tree and grasses).

Land use change in MAgPIE comes from conversion of forest land to cropland to satisfy the bioenergy demand resulting in a significant increase in the land related emissions as illustrated in Figure 12 and Figure 13. the higher the price offered for biomass, the higher the land use change amount is (Figure 12) and the higher the emissions from land use change become (Figure 13).

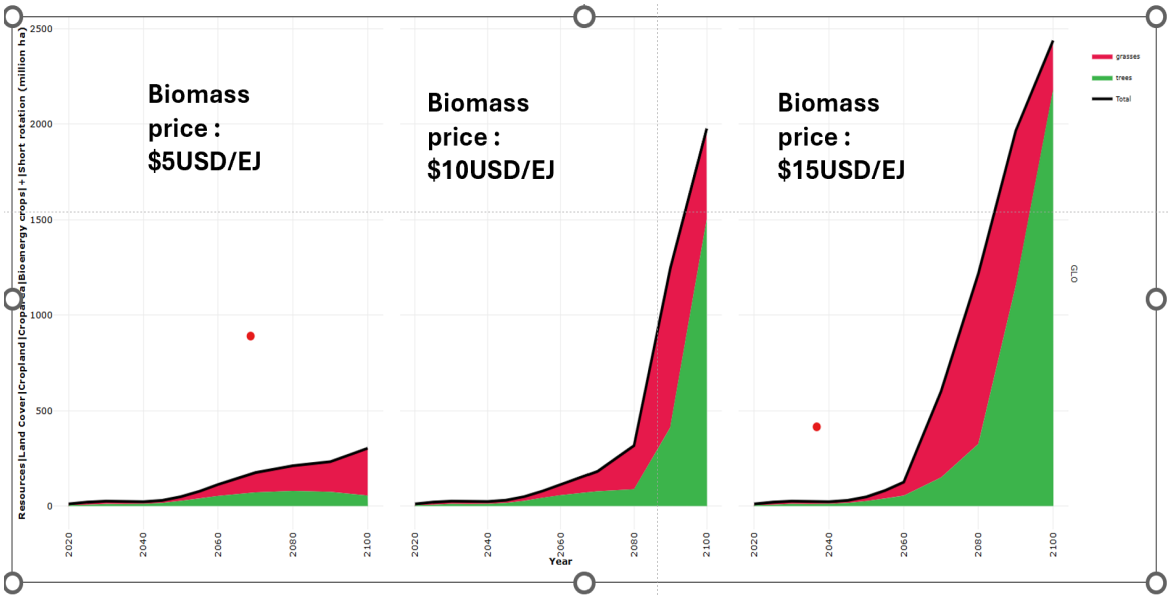

Figure 12. Land expansion of 2nd generation energy crops: trees (green shade) and grasses (red shade) in different biomass prices scenarios.

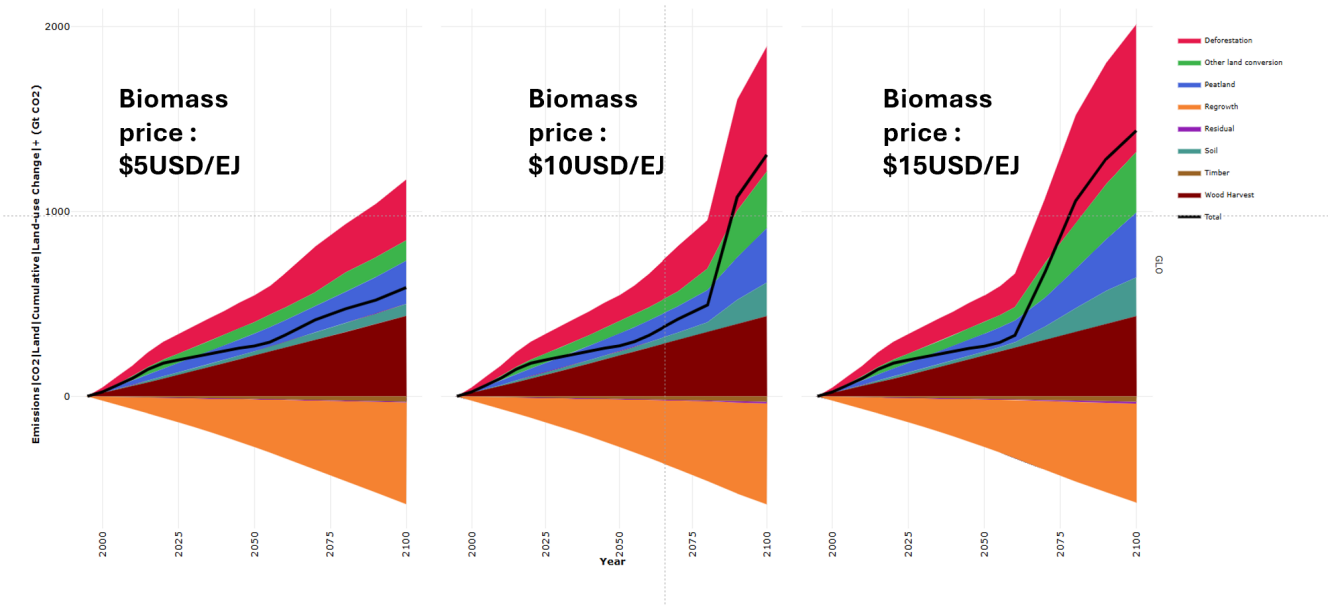

Figure 13. Cumulative land use change emissions in different biomass prices scenarios showing CO_2 sequestration by natural regrowth (orange shade) and timber plantations (brown shade), and GHG emissions from wood harvest (dark red), soil emissions (dark green), peatland loss (blue), other land conversion (green) and deforestation (red shade).

4 Soft-Linking & Integration of OPEN-PROM and MAgPIE

4.1 Introduction to MAgPIE and the need to link to OPEN-PROM

Addressing the climate crisis requires integrated insights across energy, land, and economic systems. Traditional energy system models, when used in isolation, often lack feedback from land-use dynamics caused by climate action, which can result in unrealistic assumptions on bioenergy availability, mitigation costs, and emission pathways. Similarly, land-use models frequently rely on externally defined energy demand projections and carbon pricing trajectories, limiting their responsiveness to policy changes in the energy domain. To overcome these limitations, the integration of energy-economy and land-use models has become a pressing need in integrated assessment modelling (IAM) and climate policy support (Kriegler et al., 2017; van Vuuren et al., 2011).

As is the case with the OMNIA-MAgPIE link, the integration between OPEN-PROM and MAgPIE directly responds to this challenge by bridging two independently developed models: OPEN-PROM, which simulates long-term global energy system evolution under varying climate policies, socioeconomic assumptions, and technological conditions, and MAgPIE, which captures land-use dynamics, bioenergy supply potential, and agriculture-induced emissions. This coupling enhances the realism, internal consistency, and policy relevance of scenario analyses—particularly in domains such as carbon dioxide removal (CDR), land-based mitigation, and sustainable biomass deployment.

The soft link enables bidirectional information flow and shared assumptions between the two models. The two main interactions are:

- Bioenergy demand and supply and biomass supply costs
- Carbon pricing and land use carbon emissions

OPEN-PROM provides region-specific bioenergy demand needed by the energy system and policy-driven carbon prices to MAgPIE. In response, MAgPIE endogenously determines biomass supply costs, prices and CO_2 emissions from agriculture, forestry, and other land use (AFOLU) sectors. These outputs are fed back into OPEN-PROM to update energy system developments, costs, and emissions trajectories.

This iterative exchange allows each model to influence the other's domain without fully merging them, preserving model independence while enhancing systemic coherence. As integrated assessment continues to evolve in the face of mounting climate challenges and sustainability goals (IPCC, 2022), soft-linking modelling frameworks such as this become critical tools for credible policy analysis and interdisciplinary insights.

4.2 Customising MAgPIE to be compatible with OPEN-PROM

4.2.1 Regional Detail

To align the regional granularity of OPEN-PROM and MAgPIE, we redefined the MAgPIE regional aggregation to match the 37-region configuration used in OPEN-PROM (see Figures 14 and 15). This ensures that regional energy system dynamics, biomass demand, and emissions constraints are spatially consistent. Notably, some smaller regions in MAgPIE, such as Japan, South Korea, and Taiwan, were grouped together to better align with the regional structure of OPEN-PROM, similar to the approach taken in the link with OMNIA.

Full.Country.Name	ISO3.Code	OPEN-PROM	MAgPIE	Clusters
Aruba	ABW	LAM	LAM	26
Afghanistan	AFG	OAS	OAS	16
Angola	AGO	SSA	SSA	32
Anguilla	AIA	LAM	LAM	26
Aland Islands	ALA	ELL	EUR	10
Albania	ALB	NEU	NEU	9
Andorra	AND	NEU	NEU	9
United Arab Emirates	ARE	MEA	MEA	21
Argentina	ARG	LAM	LAM	26
Armenia	ARM	REF	REF	23
American Samoa	ASM	OAS	OAS	16
Antarctica	ATA	LAM	LAM	26
French Southern Territories	ATF	OAS	OAS	16

Figure 14. Geographical mapping of OPEN-PROM regions in MAgPIE regions including the number of original clusters in each region and their respective ISO3 code.

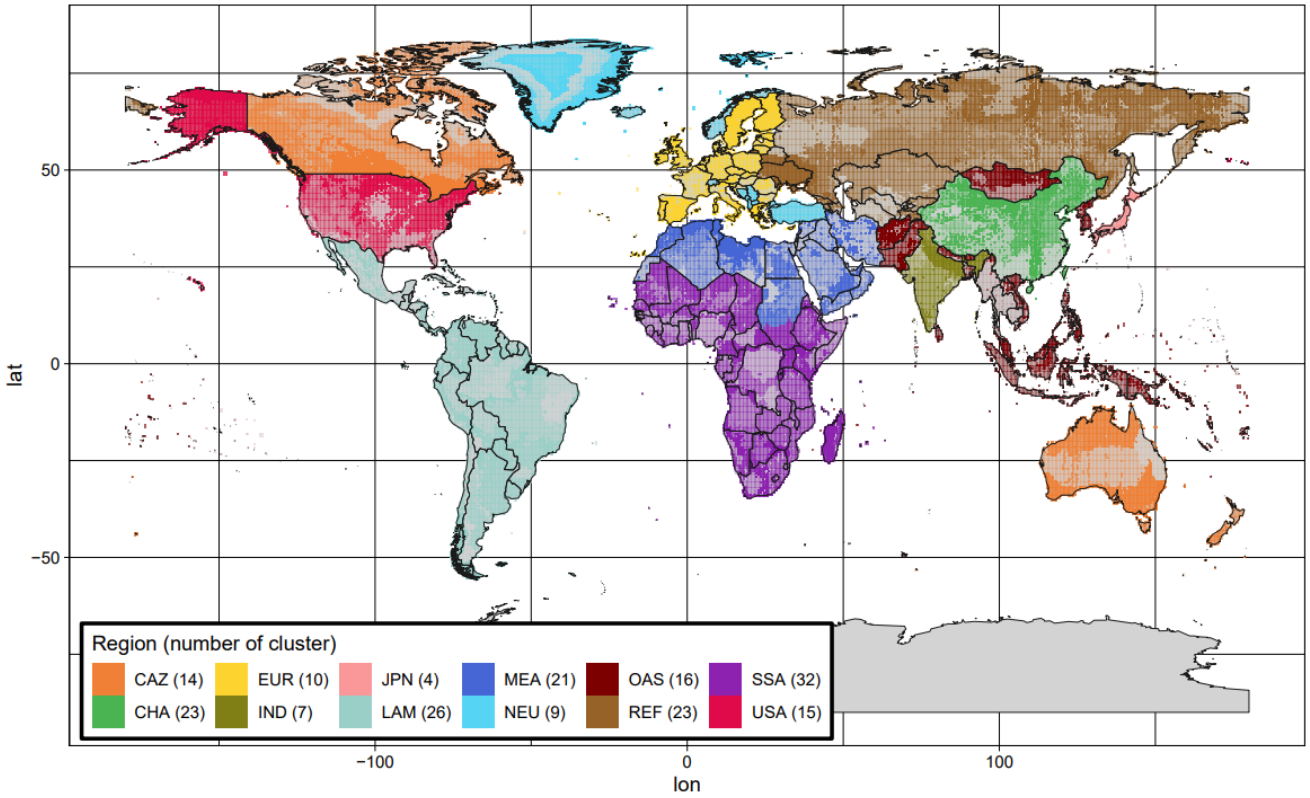

Figure 15. Geographical representation of OPEN-PROM regions in MAgPIE including the number of original clusters in each region

4.2.2 Socio-economic settings

Socioeconomic assumptions in both models were harmonised using the latest update of the Shared Socioeconomic Pathways (SSPs). Specifically, SSP2 ("middle-of-the-road") was selected as the reference scenario framework to ensure consistency in population growth, GDP trajectories, and global development narratives across both OPEN-PROM and MAgPIE. MAgPIE's internal input files were updated accordingly, with revised population and GDP drivers aligned to match the values and assumptions used in OPEN-PROM scenarios.

In addition to this harmonisation, custom scenario scripts were developed within MAgPIE to facilitate the soft-link implementation. These scripts automate the loading of scenario-specific inputs, including pollutant prices and bioenergy demands, as generated by OPEN-PROM. Three distinct policy scenarios were implemented under the SSP2 umbrella: a reference "National Policies Implemented" (NPI) scenario based on the continuation of current climate policies and energy-emission trends, and two climate mitigation pathways targeting 1.5°C and 2°C long-term temperature goals in line with the Paris Agreement goals. Each of these scenarios includes appropriate socio-economic and climate policy narratives, ensuring coherent scenario simulations across both the energy-economic and land-use domains.

4.3 Mapping OPEN-PROM outputs to MAgPIE inputs

The soft-link facilitates the transfer of two key variables from the OPEN-PROM energy-economy model to the MAgPIE land-use model:

- **Region-specific carbon prices**, which serve as economic signals for land-based mitigation efforts within MAgPIE. These prices influence decisions related to afforestation, land-use change, and emission reductions in the AFOLU sector.
- **Final bioenergy demand projections**, particularly for solid biomass, which inform the land-use allocation decisions in MAgPIE. This ensures that bioenergy demand from the energy system is met in a sustainable, cost-efficient and spatially feasible way.

These variables are extracted from the GDX outputs of OPEN-PROM and then reformatted into .cs3 files, which conform to MAgPIE's required input structure. This process is fully automated via an R-based script, ensuring reproducibility and consistency across scenario runs.

The automation script performs the following actions:

- Aggregates OPEN-PROM variables to MAgPIE's regional structure using harmonised region mapping tables.
- Interpolates values to fill missing years and adjusts temporal resolution to match MAgPIE's 5-year step format.
- Converts units as needed (e.g., bioenergy demand from Mtoe to PJ).
- Formats and writes the processed data into MAgPIE-compatible .cs3 files, namely:
    - f56_pollutant_prices.cs3 *for carbon pricing*.
    - f60_1stgen_bioenergy_dem.cs3 *for bioenergy demand*.

This setup allows OPEN-PROM to drive land-based decisions in MAgPIE under consistent climate, economic, and energy scenarios, ensuring coherent policy simulation across models.

4.3.1 Procedure for MAgPIE data extraction for OPEN-PROM

After MAgPIE completes its scenario run using the inputs from OPEN-PROM, two critical outputs are extracted and passed back to the OPEN-PROM energy model to close the feedback loop:

- **Biomass supply costs**, representing endogenous bioenergy prices based on land productivity, biophysical constraints, and policy settings in MAgPIE. These values are converted from USD17MER/GJ to k$2015/toe using standard energy unit conversions and then integrated into OPEN-PROM's fuel price input table.

- **CO_2 emissions from land-use change and agriculture**, which are used to update and complete the total GHG emissions accounting in OPEN-PROM. These emissions are essential to ensure a full-system assessment of mitigation pathways to ensure compliance with the Paris temperature goals.

The extraction is performed through a tailored R routine that reads MAgPIE's report.mif file and outputs OPEN-PROM-ready CSVs.

4.3.2 Data Exchange Between OPEN-PROM and MAgPIE

From OPEN-PROM to MAgPIE:

- Carbon Prices: Regional carbon price trajectories over time, guiding GHG mitigation in land sectors.
- Bioenergy Demand: Regional biomass demand, converted from Mtoe to PJ, guiding land allocation for energy crops and residue utilization.

From MAgPIE to OPEN-PROM:

- Biomass Costs: Regional supply-side prices for bioenergy, informing technology choices and fuel switching in OPEN-PROM.
- Land-Use CO_2 Emissions: Aggregated emissions from agriculture and land-use change, integrated into OPEN-PROM's GHG emissions accounting.

Technical Implementation

The soft link operates under a sequential run configuration, structured as:

- First OPEN-PROM Run: Generates region-specific biomass demand and carbon prices.
- MAgPIE Run: Receives these inputs, runs its internal optimization routines, and returns biomass supply costs and land-use-related CO_2 emissions.
- Second OPEN-PROM Run: Integrates the new biomass prices and land-use-related CO_2 emissions into its internal data structure and re-solves the model accordingly.

This exchange is facilitated by a custom-built R script, which is uploaded in GitHub under the following repository: linkPromToMagpie.R, and is part of the postprom toolset.

By automating both directions of the data exchange, the soft link ensures robust and replicable integration between the two models, enabling aligned scenario exploration without compromising each model's internal structure.

4.4 Preliminary results

Initial test runs have confirmed that the soft-linking mechanism between OPEN-PROM and MAgPIE operates as intended. Region-specific carbon prices and bioenergy demand projections generated by OPEN-PROM were successfully passed to MAgPIE, with the latter model then responding with consistent outputs on biomass prices and land-use CO_2 emissions. These results were reintegrated into OPEN-PROM to complete the soft-link cycle. For validation purposes, CO_2 emissions from the AFOLU sector were benchmarked against externally sourced trajectories derived from the NAVIGATE project (https://iiasa.ac.at/projects/navigate), based on the REMIND-MAgPIE 3_2-4_6 scenario framework. These externally provided emissions pathways—used as exogenous inputs in the stand-alone OPEN-PROM version and depicted in green in the figures below—serve as a reference to verify that MAgPIE reacts correctly to policy signals from the energy model. The results from the three climate policy scenarios (NPi, 2°C, and 1.5°C) confirm that the soft link yields coherent, credible differentiated land-based

mitigation outcomes across alternative levels of mitigation ambition/stringency, providing evidence of proper directional data flow and functional integration. Germany and the USA were selected as test cases due to their highly industrialised economies, substantial land-use emissions potential, and ambitious climate mitigation targets, including strong reliance on negative emissions pathways—making them ideal for evaluating both the robustness and sensitivity of the soft-linked modelling framework.

First, as a comparison between the OPEN-PROM and the OPEN-PROM–MAgPIE soft link, the results of "Bioenergy Price | Final Energy" are presented, one for each SSP2 scenario and for the following climate policy/temperature targets: Figure 16-NPi, Figure 17-2C and Figure 18-1p5C, for the countries of Germany (DEU) and United States of America (USA).

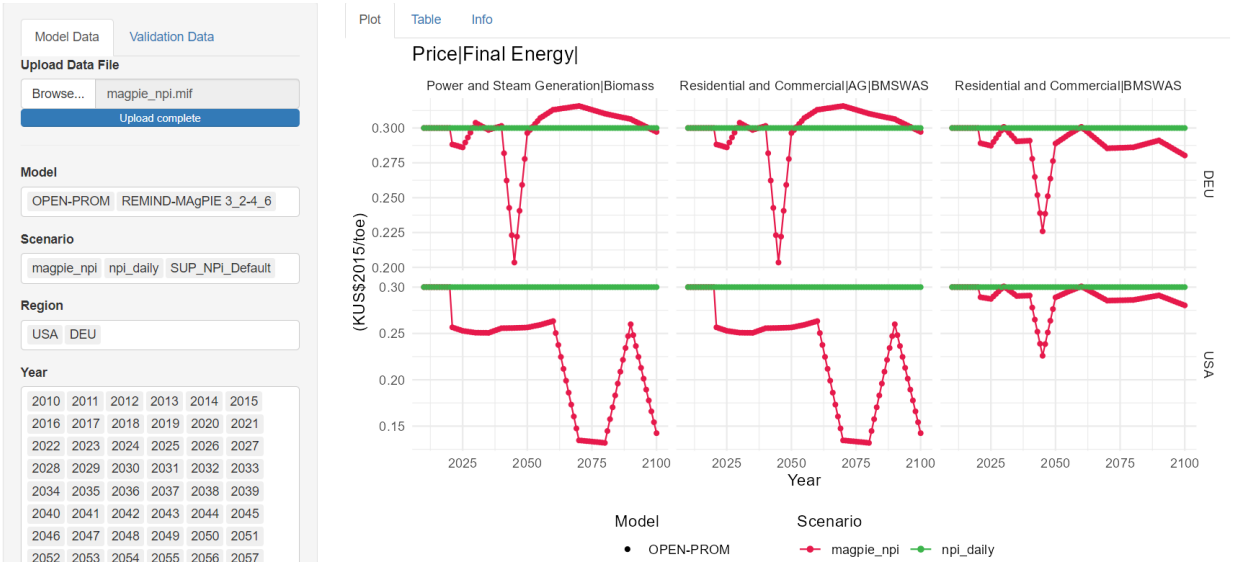

Figure 16. Bioenergy Price | Final Energy SSP2- NPi scenario.

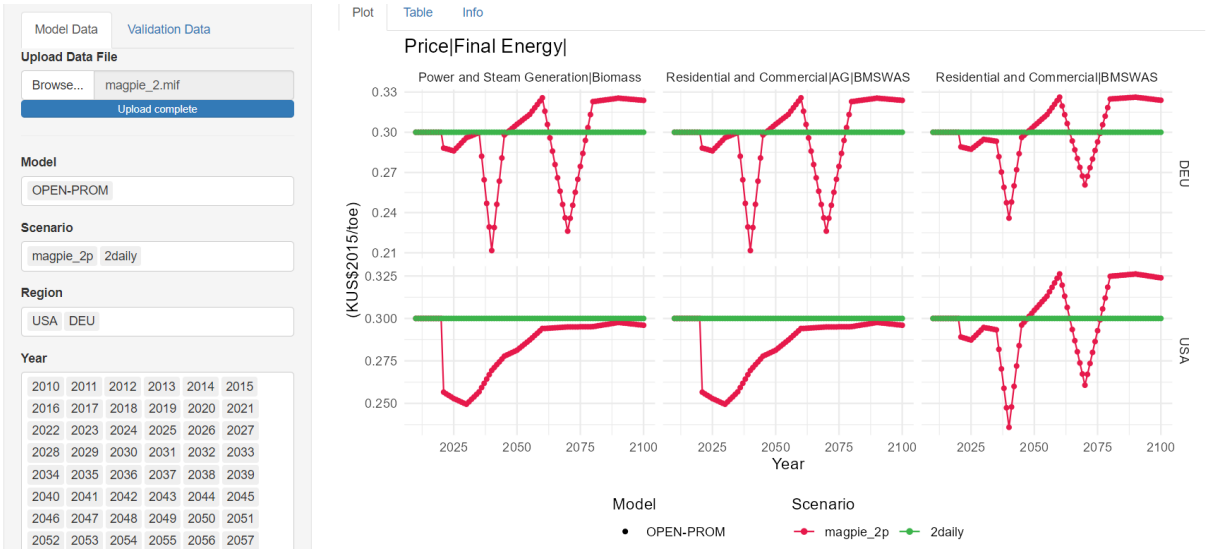

Figure 17. Bioenergy Price | Final Energy SSP2- 2C scenario.

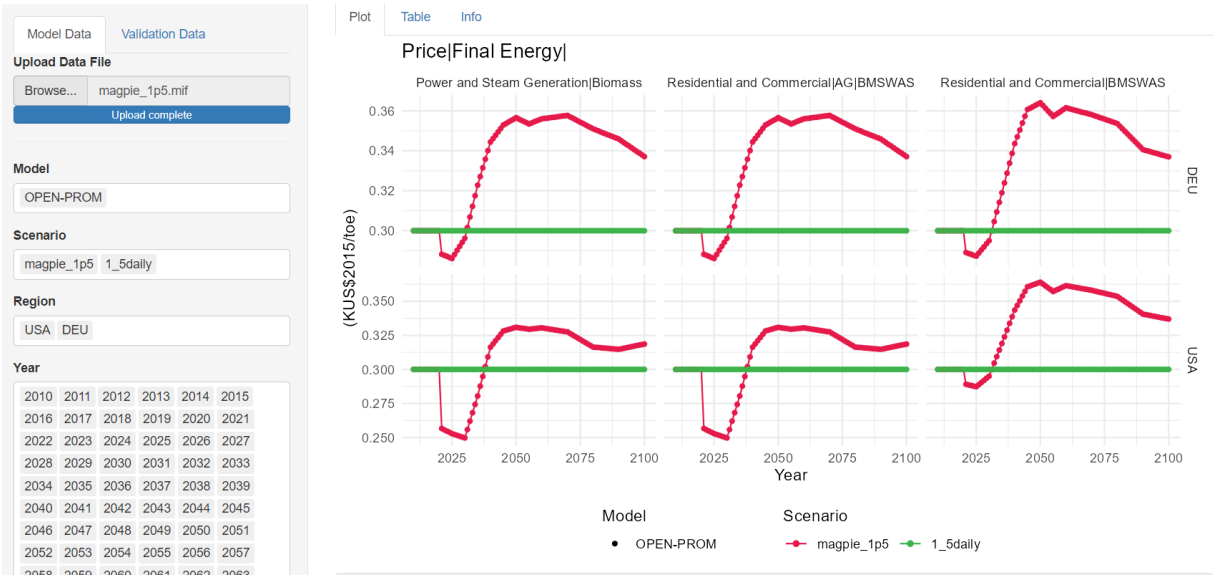

Figure 18. Bioenergy Price | Final Energy SSP2- 1p5C.

Furthermore, as a comparison between the OPEN-PROM and the OPEN-PROM–MAgPIE soft link, the results of the "CO2 Emissions | AFOLU" are presented, one for each SSP2 scenario and for the following climate policy/temperature targets: Figure 19-NPi, Figure 20-2C and Figure 21-1p5C, for the countries of Germany (DEU) and United States of America (USA).

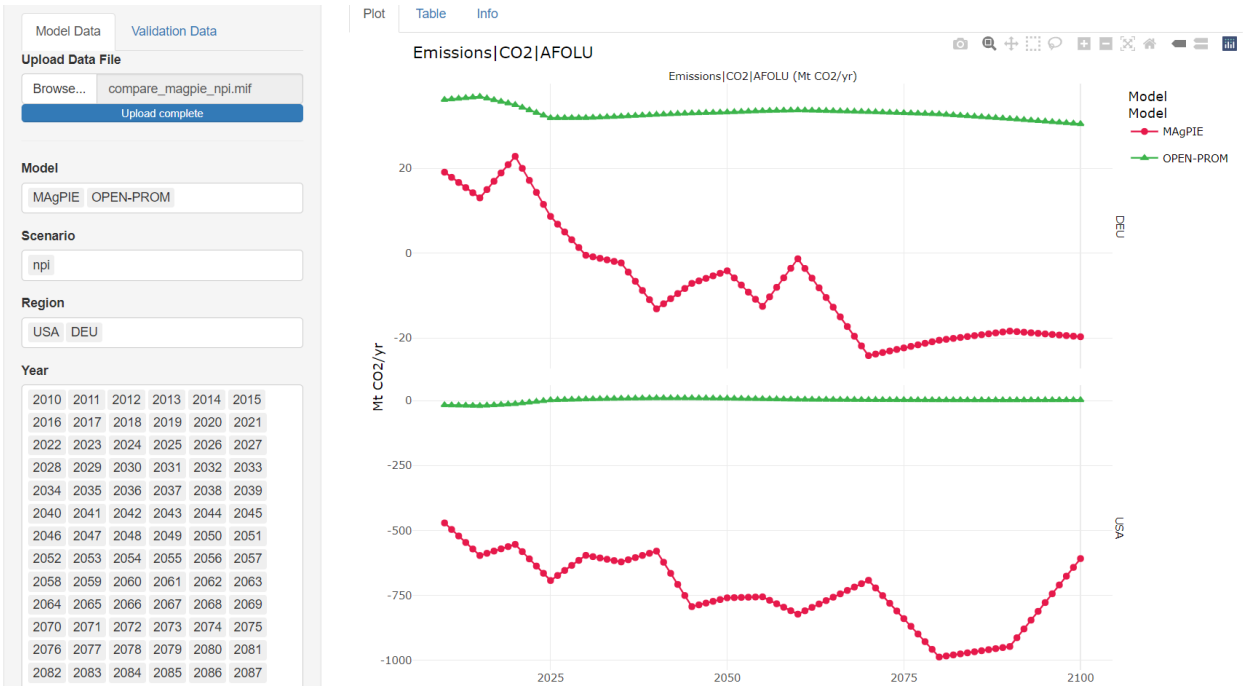

Figure 19. CO_2 Emissions from the AFOLU sector in the SSP2- NPi scenario.

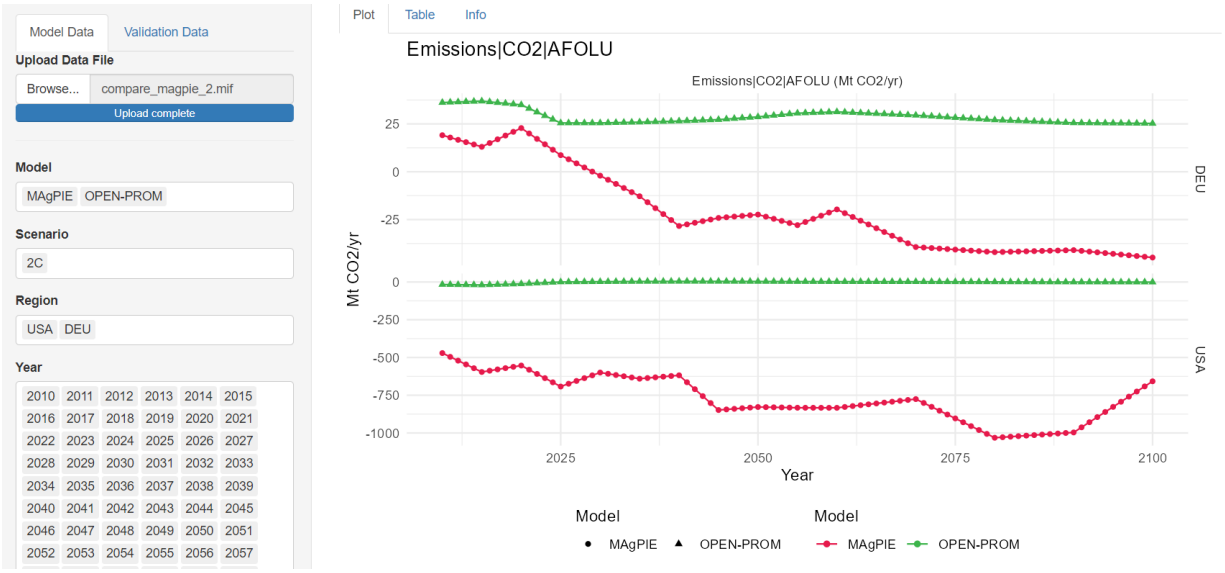

Figure 20. CO_2 Emissions from the AFOLU sector in the SSP2- 2C scenario.

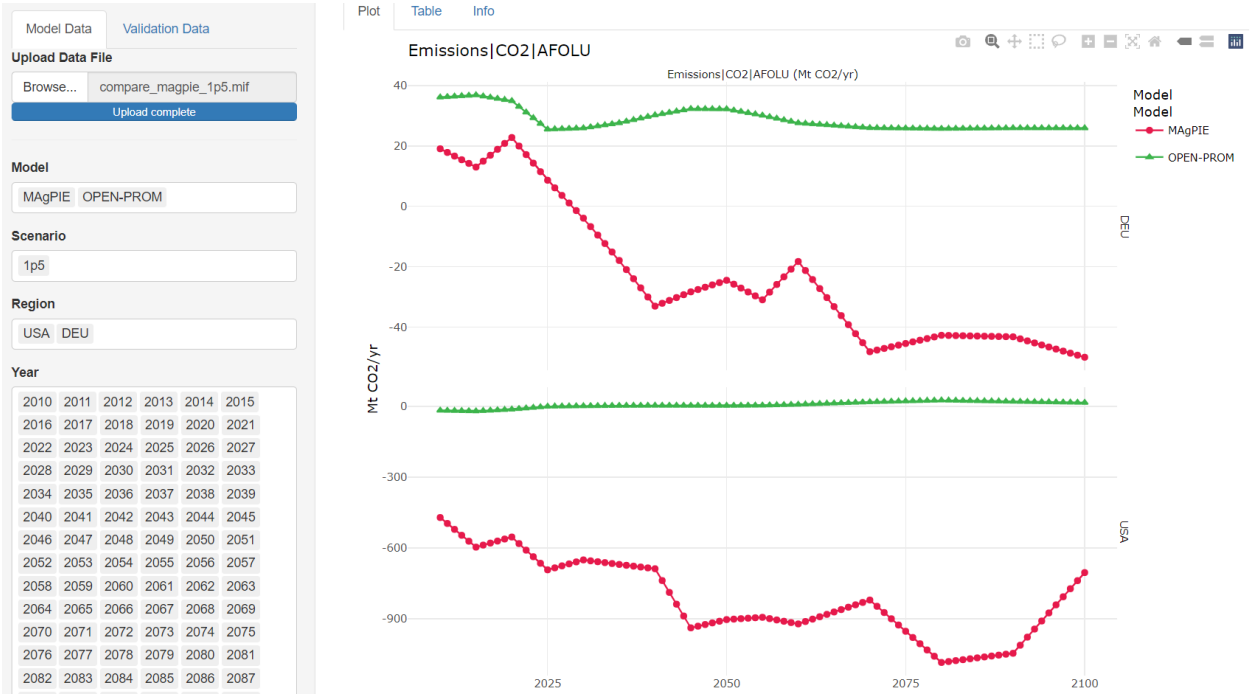

Figure 21. CO2 Emissions from the AFOLU sector in the SSP2- 1p5C scenario.

Lastly, the comparison of the results of the soft link of OPEN-PROM – MAgPIE between the 3 different climate policy scenarios (NPi, 2C and 1p5C) for the countries of Germany (DEU) and United States of America (USA) are presented, in the Figure 22 and Figure 23, below.

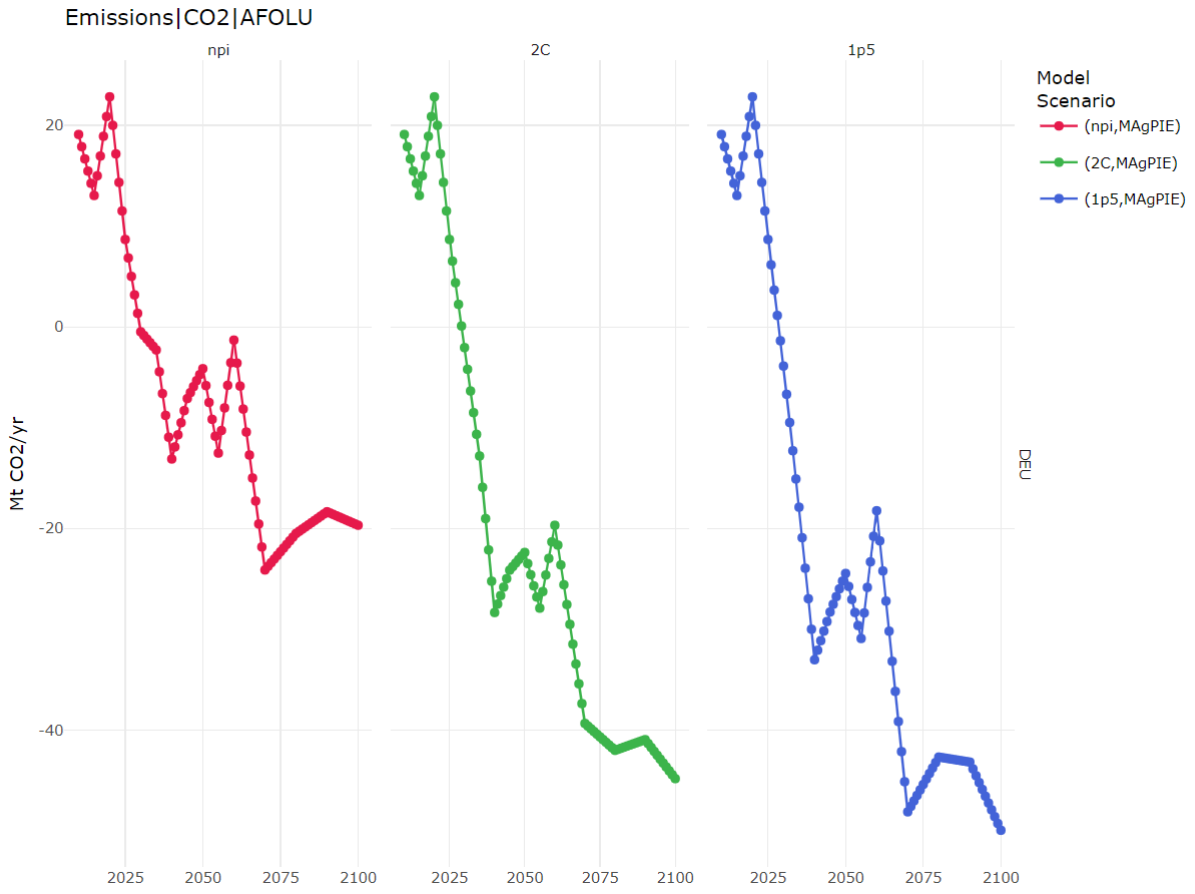

Figure 22. CO_2 Emissions from the AFOLU sector in the alternative climate policy scenarios for Germany (DEU).

The AFOLU CO_2 emissions, in Figure 22, show a significant differentiation between climate ambition levels. Under the **NPi** scenario, emissions initially decline but fluctuate around net-zero levels after 2050, stabilising close to -20 $MtCO_2$/year by 2100. This suggests limited emissions reduction in the land use sector, with modest afforestation. In the **2°C scenario**, emissions drop steeply after 2030, reaching approximately -40 Mt CO_2/year post-2080. This reflects enhanced land-based mitigation, likely involving reforestation and reduced agricultural emissions. The **1.5°C scenario** demonstrates the strongest emissions reduction, with a sharp drop beginning before 2030, reaching around -50 Mt CO_2/year by century's end. The deep negative emissions trajectory in this pathway aligns with more aggressive afforestation and sustainable land management to offset residual emissions from other hard-to-abate sectors and meet stringent climate targets.

Funded by
the European Union

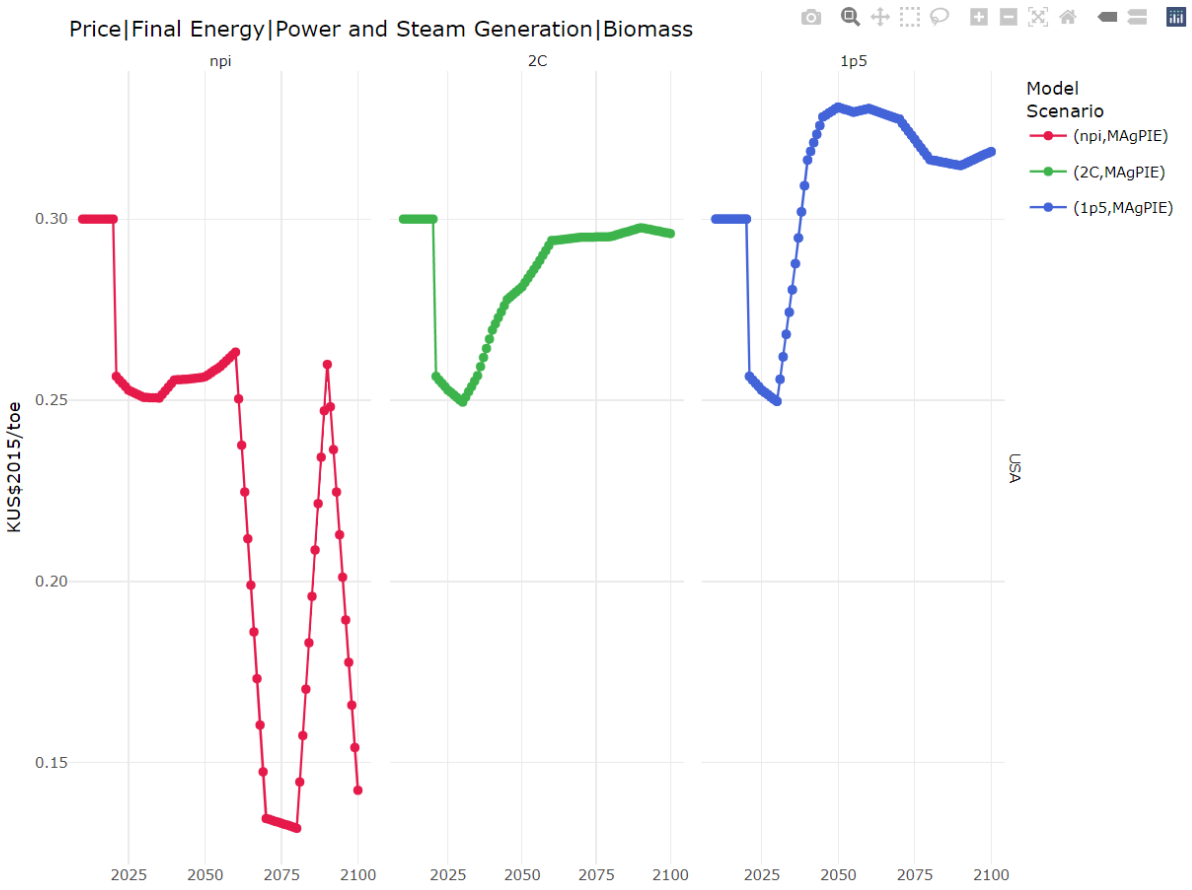

Figure 23. Bioenergy Price | Final Energy between the SSP2 scenarios for USA.

The trends in Figure 23, reveal clear distinctions between the three scenarios. In the **NPi** pathway, biomass prices begin around 0.30 k$2015/toe and experience a significant drop after 2070, falling below 0.15 k$2015/toe. This decline reflects reduced long-term pressure on bioenergy demand and land competition due to the absence of stricter climate policy and improved land/agriculture management. In the **2°C scenario**, biomass prices remain relatively stable around 0.26–0.29 k$2015/toe (at much higher values compared to NPi) but exhibit a gradual increase until 2080, indicating increasing global biomass demand driven by decarbonization efforts. The **1.5°C scenario** shows the highest and most volatile price levels, peaking above 0.32 k$2015/toe between 2040 and 2080. This represents a rise of over 60% compared to estimated 2020 biomass price levels (around 0.20 k$2015/toe), and exceeds the upper bounds of historical biomass price volatility, which typically ranged between 0.10–0.25 k$2015/toe. This reflects the intensification of mitigation action, where strong carbon pricing mechanisms leads to high biomass demand (in OPEN-PROM) that results in increased land-use competition and consequently higher costs and prices for biomass.

The comparison of scenario results across the SSP2-NPi, 2°C, and 1.5°C pathways demonstrates that the soft-link between OPEN-PROM and MAgPIE is functioning as intended. Under stricter climate scenarios, both biomass prices (exemplified for the USA) and AFOLU CO_2 emissions (exemplified for Germany) respond in a directionally consistent manner: higher decarbonisation ambition leads to increased biomass costs due to rising biomass demand and land competition, while CO_2 emissions from land use become increasingly negative, reflecting stronger afforestation and mitigation efforts. These dynamics confirm that policy signals—carbon prices and bioenergy demand—from OPEN-PROM are correctly received and interpreted by MAgPIE, and that feedbacks such as biomass supply costs and land-use emissions are properly returned to OPEN-PROM via the soft-link approach. The observed trajectories provide strong evidence that the models are exchanging data coherently and the sequential linkage is producing integrated, policy-sensitive outcomes.

Funded by
the European Union

5 Conclusions & Next Steps

5.1 MAgPIE Dietary Risk Module Conclusions & Next Steps

The current demand module outputs of The Model of Agricultural Production and its Impact on the Environment (MAgPIE) are sufficient inputs for a dietary risk module, which attributes disease burden measured in years of life lost (mortality), and years of life lost to disease (morbidity) to population exposure to underweight or overweight and dietary composition. The large disease burden associated to current diets and responses to land-use changes, greenhouse gas emission changes, and consumption trends will be able to be estimated and incorporated into integrated modelling using the dietary risk module outputs.

The demand module outputs require translation to the required inputs for Global Burden of Disease model emulators, and future work beyond the DIAMOND could investigate bridging the MAgPIE demand module output into finer resolution of population intake to better match the exposure variables of emulators. Forecasting total disease burden rates into the future is an extensive and specialist task, currently conducted by a team at the IMHE that hosts the Global Burden of Disease study. Future improvements could also link the exogenous and economic projections from MAgPIE and integrated models closer to the total disease burden forecasts. At present, for the first version of the dietary risk module, transformation of the GBD forecasts using available demographic information in exogenous projections driving MAgPIE is the simple and pragmatic option. The GBD forecasts are only available to 2050 and after this date extrapolations would be required to predict further to 2100 or 2150.

The next steps for building the first version of the dietary risk module will be technical coding work, to pair the current instantiation of GBD emulators written in Python and create a pipeline for calculations with a standard package of MAgPIE. This work will inform the ability of the dietary risk module to incorporate uncertainty estimates coming from the emulator model components in outputs.

5.2 OMNIA – MAgPIE Conclusions & Next Steps

The soft linking of MAgPIE to the new OMNIA model demonstrated that a soft-link approach is feasible, improving the biomass resource representation in open-source energy models. Currently, the soft-link MAgPIE-OMNIA only used SSP2 – NDC settings, but it demonstrated feasibility, and it can be replicated to analyse biomass feedstock results and related emissions in other SSPs and other policies than NDCs.

Based on the discussions on stakeholder feedback earlier this year and additional model development improvements, activities employing the MAgPIE-OMNIA in WP5 may require further adjustments of key parameters to be extracted from MAgPIE and used in OMNIA—e.g., for now MAgPIE only considers CO_2 fertilisation due to climate change, but based on stakeholder requests, we might also need to include temperature change impacts on yields, as CO_2 fertilisation effect is endogenous included in the MAgPIE model. In the next steps, we will iteratively exchange the CO_2 prices and demand from OMNIA scenario runs to MAgPIE and afforestation and land use emissions to OMNIA to understand the effects of land use change uncertainties on the transition pathways.

Biodiversity representation in MAgPIE is currently limited to one indicator, namely BII (Biodiversity Intactness Index), which estimates how much of the natural ecosystems remain after human impacts. We could use this indicator results to illustrate biodiversity impacts of transition pathways, as requested in stakeholder workshops.

5.3 OPEN-PROM – MAgPIE Conclusions & Next Steps

This work has demonstrated the feasibility and validity of a soft-linking approach between the OPEN-PROM

Funded by
the European Union

energy system model and the MAgPIE land-use model. Through this linkage, crucial variables such as bioenergy demand and carbon prices were successfully transferred from the energy to the land-use domain, while resulting biomass prices and land-use CO_2 emissions were reintegrated into the energy model. The coordinated scenario runs under NPi, 2°C, and 1.5°C climate targets have shown that the soft-link yields consistent and directionally correct results, enabling coherent cross-sectoral assessments.

Building on this, future work could focus on introducing iterative feedback loops between the models to better capture dynamic interactions over time. The scope of exchanged variables can also be broadened to include, for instance, land availability constraints, negative emissions potentials, and ecosystem service trade-offs. Furthermore, efforts will be directed toward refining the regional and technological mappings to enhance the spatial and sectoral granularity of the exchange.

Beyond technical improvements, this soft-linking work holds great promise in informing more holistic, policy-relevant scenarios that reflect real-world interdependencies between energy, land, and climate systems. Potential extensions include the integration of biodiversity constraints and indicators, in line with emerging EU and global policy priorities, and support for richer policy packages combining energy, land use, and nature-based solutions. This approach ultimately enables more robust assessments of climate strategies that are consistent, realistic, and aligned with the twin objectives of decarbonisation and biodiversity protection.

5.4 Overall conclusions and next steps

Recent developments across the MAgPIE modelling framework have significantly expanded its capacity to assess interconnected sustainability challenges. The newly developed Dietary Risk Module enhances MAgPIE by enabling the quantification of health impacts associated with dietary patterns, providing a basis to estimate disease burdens from undernutrition, overnutrition, and dietary composition. This represents a genuinely novel achievement by linking land-use dynamics directly to health outcomes. Next steps involve technical implementation to integrate Global Burden of Disease model emulators and refine demographic inputs for more precise exposure estimates. In parallel, the soft-linking of MAgPIE with the OPEN-PROM energy model has proven effective, enabling consistent cross-sectoral analyses of land-use and energy systems through shared variables such as bioenergy demand and carbon prices. This technically demanding work required automated data exchange and the resolution of regional aggregation challenges across distinct modelling frameworks. Future work will develop iterative feedbacks and broaden the scope of exchanged variables. Similarly, the MAgPIE-OMNIA soft-link has shown feasibility in improving biomass and land-use emission representation, with further refinements needed to align assumptions, integrate climate impact factors on yields, and enhance biodiversity metrics. Together, these advancements represent ambitious, interdisciplinary progress in bridging land, energy, health, and economic systems, and position MAgPIE as a more comprehensive and policy-relevant tool. While significant progress has been made, this remains important foundational work, with further validation and refinement needed to fully realise the potential of these integrated modelling capabilities.

Funded by
the European Union

References

Afshin, A., Sur, P. J., Fay, K. A., Cornaby, L., Ferrara, G., Salama, J. S., Mullany, E. C., Abate, K. H., Abbafati, C., & Abebe, Z. (2019). Health effects of dietary risks in 195 countries, 1990–2017: a systematic analysis for the Global Burden of Disease Study 2017. The Lancet, 393(10184), 1958-1972.

Bauer, N., Klein, D., Humpenöder, F. et al. Bio-energy and CO2 emission reductions: an integrated land-use and energy sector perspective. Climatic Change 163, 1675–1693 (2020). https://doi.org/10.1007/s10584-020-02895-z

Baumstark, L., Bauer, N., Benke, F., Bertram, C., Bi, S., Gong, C. C., Dietrich, J. P., Dirnaichner, A., Giannousakis, A., Hilaire, J., Klein, D., Koch, J., Leimbach, M., Levesque, A., Madeddu, S., Malik, A., Merfort, A., Merfort, L., Odenweller, A.,...Luderer, G. (2021). REMIND2.1: transformation and innovation dynamics of the energy-economic system within climate and sustainability limits. Geosci. Model Dev., 14(10), 6571-6603. https://doi.org/10.5194/gmd-14-6571-2021

Beal, T., Herforth, A., Sundberg, S., Hess, S. Y., & Neufeld, L. M. (2021). Differences in modelled estimates of global dietary intake. The Lancet, 397(10286), 1708-1709. https://doi.org/10.1016/S0140-6736(21)00714-5

Beal, T., Neufeld, L. M., & Morris, S. S. (2019). Uncertainties in the GBD 2017 estimates on diet and health. The Lancet, 394(10211), 1801-1802. https://doi.org/10.1016/S0140-6736(19)32502-4

Bodirsky, B. L., Dietrich, J. P., Martinelli, E., Stenstad, A., Pradhan, P., Gabrysch, S., Mishra, A., Weindl, I., Le Mouël, C., Rolinski, S., Baumstark, L., Wang, X., Waid, J. L., Lotze-Campen, H., & Popp, A. (2020). The ongoing nutrition transition thwarts long-term targets for food security, public health and environmental protection. Scientific Reports, 10(1), 19778. https://doi.org/10.1038/s41598-020-75213-3

Dai, H., Alsalhe, T. A., Chalghaf, N., Riccò, M., Bragazzi, N. L., & Wu, J. (2020). The global burden of disease attributable to high body mass index in 195 countries and territories, 1990–2017: An analysis of the Global Burden of Disease Study. PLOS Medicine, 17(7), e1003198. https://doi.org/10.1371/journal.pmed.1003198

Dietrich J, Bodirsky B, Weindl I, Humpenöder F, Stevanovic M, Kreidenweis U, Wang X, Karstens K, Mishra A, Beier F, Molina Bacca E, von Jeetze P, Windisch M, Crawford M, Leip D, Klein D, Singh V, Ambrósio G, Araujo E, Biewald A, Sauer P, Köberle A, Steinhauser J, Hötten D, Lotze-Campen H, Popp A (2024). "MAgPIE - An Open Source land-use modeling framework - Version 4.8.2." doi:10.5281/zenodo.1418752 https://doi.org/10.5281/zenodo.1418752 , https://github.com/magpiemodel/magpie

Dietrich, J. P., Bodirsky, B. L., Humpenöder, F., Weindl, I., Stevanović, M., Karstens, K., Kreidenweis, U., Wang, X., Mishra, A., & Klein, D. (2019). MAgPIE 4–a modular open-source framework for modeling global land systems. Geoscientific Model Development, 12(4), 1299-1317.

Dietrich, Jan Philipp, Christoph Schmitz, Hermann Lotze-Campen, Alexander Popp, and Christoph Müller. 2014. "Forecasting Technological Change in Agriculture—an Endogenous Implementation in a Global Land Use Model." Technological Forecasting and Social Change 81: 236–49. https://doi.org/10.1016/j.techfore.2013.02.003.

E3Modelling. (2024). linkPromToMagpie.R: Automation script for soft-linking OPEN-PROM and MAgPIE [R script]. GitHub. https://github.com/e3modelling/OPEN-PROM

E3Modelling. (2024). OPEN-PROM energy model [Computer software]. GitHub. https://github.com/e3modelling/OPEN-PROM

Evangelopoulos, D., Perez-Velasco, R., Walton, H., Gumy, S., Williams, M., Kelly, F. J., & Künzli, N. (2020). The role

of burden of disease assessment in tracking progress towards achieving WHO global air quality guidelines. International Journal of Public Health, 65(8), 1455-1465. https://doi.org/10.1007/s00038-020-01479-z

Ferrari, A. J., Santomauro, D. F., Aali, A., Abate, Y. H., Abbafati, C., Abbastabar, H., Abd ElHafeez, S., Abdelmasseh, M., Abd-Elsalam, S., Abdollahi, A., Abdullahi, A., Abegaz, K. H., Abeldaño Zuñiga, R. A., Aboagye, R. G., Abolhassani, H., Abreu, L. G., Abualruz, H., Abu-Gharbieh, E., Abu-Rmeileh, N. M. E.,...Murray, C. J. L. (2024). Global incidence, prevalence, years lived with disability (YLDs), disability-adjusted life-years (DALYs), and healthy life expectancy (HALE) for 371 diseases and injuries in 204 countries and territories and 811 subnational locations, 1990-2021: a systematic analysis for the Global Burden of Disease Study 2021. The Lancet, 403(10440), 2133-2161. https://doi.org/10.1016/S0140-6736(24)00757-8

Global Burden of Disease Collaborative Network. (2018). Global Burden of Disease Study 2017 (GBD 2017) Results [Database]. http://ghdx.healthdata.org/gbd-2017

Harker, D., Harker, M., & Svensen, S. (2007). Attributing Blame. Journal of Food Products Marketing, 13(2), 33-46. https://doi.org/10.1300/J038v13n02_03

Intergovernmental Panel on Climate Change (IPCC). (2022). Climate Change 2022: Synthesis Report. Contribution of Working Groups I, II and III to the Sixth Assessment Report of the Intergovernmental Panel on Climate Change. IPCC. https://www.ipcc.ch/report/ar6/syr/

Jan, S., & Mooney, G. H. (2006). Childhood obesity, values and the market [https://doi.org/10.1080/17477160600881312]. International Journal of Pediatric Obesity, 1(3), 131-132. https://doi.org/https://doi.org/10.1080/17477160600881312

Karnani, A., McFerran, B., & Mukhopadhyay, A. (2016). The Obesity Crisis as Market Failure: An Analysis of Systemic Causes and Corrective Mechanisms. Journal of the Association for Consumer Research, 1(3), 445-470. https://doi.org/10.1086/686244

Keywan Riahi, Detlef P. van Vuuren, Elmar Kriegler, Jae Edmonds, Brian C. O'Neill, Shinichiro Fujimori, Nico Bauer, Katherine Calvin, Rob Dellink, Oliver Fricko, Wolfgang Lutz, Alexander Popp, Jesus Crespo Cuaresma, Samir KC, Marian Leimbach, Leiwen Jiang, Tom Kram, Shilpa Rao, Johannes Emmerling, Kristie Ebi, Tomoko Hasegawa, Petr Havlík, Florian Humpenöder, Lara Aleluia Da Silva, Steve Smith, Elke Stehfest, Valentina Bosetti, Jiyong Eom, David Gernaat, Toshihiko Masui, Joeri Rogelj, Jessica Strefler, Laurent Drouet, Volker Krey, Gunnar Luderer, Mathijs Harmsen, Kiyoshi Takahashi, Lavinia Baumstark, Jonathan C. Doelman, Mikiko Kainuma, Zbigniew Klimont, Giacomo Marangoni, Hermann Lotze-Campen, Michael Obersteiner, Andrzej Tabeau, Massimo Tavoni. The Shared Socioeconomic Pathways and their energy, land use, and greenhouse gas emissions implications: An overview, Global Environmental Change, Volume 42, Pages 153-168, 2017, ISSN 0959-3780, DOI:110.1016/j.gloenvcha.2016.05.009

Klein, D., Luderer, G., Kriegler, E., Strefler, J., Bauer, N., Leimbach, M., Popp, A., Dietrich, J. P., Humpenöder, F., Lotze-Campen, H., & Edenhofer, O. (2014). The value of bioenergy in low stabilization scenarios: an assessment using REMIND-MAgPIE. Clim Change, 123. https://doi.org/10.1007/s10584-013-0940-z

Kriegler, E., Bauer, N., Popp, A., Humpenöder, F., Leimbach, M., Strefler, J., Baumstark, L., Bodirsky, B. L., Hilaire, J., Klein, D., Mouratiadou, I., Weindl, I., Bertram, C., Dietrich, J. P., Luderer, G., Pehl, M., Pietzcker, R. C., Piontek, F., Lotze-Campen, H., & Edenhofer, O. (2017). Fossil-fueled development (SSP5): An energy and resource intensive scenario for the 21st century. Global Environmental Change, 42, 297–315. https://doi.org/10.1016/j.gloenvcha.2016.05.015

Lescinsky, H., Afshin, A., Ashbaugh, C., Bisignano, C., Brauer, M., Ferrara, G., Hay, S. I., He, J., Iannucci, V., Marczak, L. B., McLaughlin, S. A., Mullany, E. C., Parent, M. C., Serfes, A. L., Sorensen, R. J. D., Aravkin, A. Y., Zheng, P.,

& Murray, C. J. L. (2022). Health effects associated with consumption of unprocessed red meat: a Burden of Proof study. Nature Medicine, 28(10), 2075-2082. https://doi.org/10.1038/s41591-022-01968-z

Lord, S. (2021). Estimation of marginal damage costs from water scarcity due to blue water withdrawal (Documentation of the SPIQ-FS Dataset Version 0. Annex A, Issue.

Lord, S. (2023). Comparative Hidden Costs of the Food System Economic Commission Current Trends and Food System Transformation Pathways to 2050 (Working Papers FSEC, Issue. https://foodsystemeconomics.org/science/working-papers/

Lotze-Campen, Hermann, Martin von Lampe, Page Kyle, Shinichiro Fujimori, Petr Havlik, Hans van Meijl, Tomoko Hasegawa, et al. 2014. "Impacts of Increased Bioenergy Demand on Global Food Markets: An AgMIP Economic Model Intercomparison." Agricultural Economics 45 (1): 103–16. https://doi.org/10.1111/agec.12092.

Mathers, C. D. (2020). History of global burden of disease assessment at the World Health Organization. Archives of Public Health, 78(1), 77. https://doi.org/10.1186/s13690-020-00458-3

McCarthy, M. (2004). The economics of obesity. The Lancet, 364(9452), 2169-2170. https://doi.org/10.1016/S0140-6736(04)17613-7

Moodie, R., Swinburn, B., Richardson, J., & Somaini, B. (2006). Childhood obesity – a sign of commercial success, but a market failure. International Journal of Pediatric Obesity, 1(3), 133-138. https://doi.org/10.1080/17477160600845044

Murray, C. J. L., Ezzati, M., Lopez, A. D., Rodgers, A., & Vander Hoorn, S. (2003). Comparative quantification of health risks: Conceptual framework and methodological issues. Population Health Metrics, 1(1), 1. https://doi.org/10.1186/1478-7954-1-1

Murray, C. J., Aravkin, A. Y., Zheng, P., Abbafati, C., Abbas, K. M., Abbasi-Kangevari, M., Abd-Allah, F., Abdelalim, A., Abdollahi, M., & Abdollahpour, I. (2020). Global burden of 87 risk factors in 204 countries and territories, 1990–2019: a systematic analysis for the Global Burden of Disease Study 2019. The Lancet, 396(10258), 1223-1249.

Ng, M., Dai, X., Cogen, R. M., Abdelmasseh, M., Abdollahi, A., Abdullahi, A., Aboagye, R. G., Abukhadijah, H. J., Adeyeoluwa, T. E., Afolabi, A. A., Ahmad, D., Ahmad, N., Ahmed, A., Ahmed, S. A., Akkaif, M. A., Akrami, A. E., Al Hasan, S. M., Al Ta'ani, O., Alahdab, F.,...Gakidou, E. (2024). National-level and state-level prevalence of overweight and obesity among children, adolescents, and adults in the USA, 1990–2021, and forecasts up to 2050. The Lancet, 404(10469), 2278-2298. https://doi.org/10.1016/S0140-6736(24)01548-4

Paulus, E. and S. Lord, Estimation of marginal damage costs from consumption related health risks, in SPIQ-FS Dataset Version 0. 2022, University of Oxford.

PIK – Potsdam Institute for Climate Impact Research. (2024). MAgPIE (Model of Agricultural Production and its Impact on the Environment) [Computer software]. GitHub. https://github.com/magpiemodel/magpie

SSP Scenario Explorer (SSP 3.1.0, Release January 2024). https://data.ece.iiasa.ac.at/ssp/#/about

Stanaway, J. D., Afshin, A., Gakidou, E., Lim, S. S., Abate, D., Abate, K. H., Abbafati, C., Abbasi, N., Abbastabar, H., & Abd-Allah, F. (2018). Global, regional, and national comparative risk assessment of 84 behavioural, environmental and occupational, and metabolic risks or clusters of risks for 195 countries and territories, 1990–2017: a systematic analysis for the Global Burden of Disease Study 2017. The Lancet, 392(10159),

1923-1994.

Stanton, A. V. (2024). Unacceptable use of substandard metrics in policy decisions which mandate large reductions in animal-source foods. npj Science of Food, 8(1), 10. https://doi.org/10.1038/s41538-024-00249-y

Swaminathan, S., Hemalatha, R., Pandey, A., Kassebaum, N. J., Laxmaiah, A., Longvah, T., Lodha, R., Ramji, S., Kumar, G. A., Afshin, A., Gupta, S. S., Kar, A., Khera, A. K., Mathai, M., Awasthi, S., Rasaily, R., Varghese, C. M., Millear, A. I., Manguerra, H.,...Dandona, L. (2019). The burden of child and maternal malnutrition and trends in its indicators in the states of India: the Global Burden of Disease Study 1990–2017. The Lancet Child & Adolescent Health, 3(12), 855-870. https://doi.org/10.1016/S2352-4642(19)30273-1

van Vuuren, D. P., Edmonds, J., Kainuma, M., Riahi, K., Thomson, A., Hibbard, K., Hurtt, G. C., Kram, T., Krey, V., Lamarque, J. F., Masui, T., Meinshausen, M., Nakicenovic, N., Smith, S. J., & Rose, S. K. (2011). The representative concentration pathways: An overview. Climatic Change, 109(1–2), 5–31. https://doi.org/10.1007/s10584-011-0148-z

Vittis, Y., Folberth, C., Bundle, S. C., & Obersteiner, M. (2021). Restoring nature at lower food production costs. Frontiers in Environmental Science, 9, 672663.

Vittis, Y., Mosnier, A., Smith, A., Arguelle, R., Chavarro Diaz, J., Costa, W., & Koeberle, A. (2024). What are the levers to reduce agrifood systems' future hidden costs? A multi-country case study. Background paper for The State of Food and Agriculture 2024.

Vollset, S. E., Ababneh, H. S., Abate, Y. H., Abbafati, C., Abbasgholizadeh, R., Abbasian, M., Abbastabar, H., Abd Al Magied, A. H. A., Abd ElHafeez, S., Abdelkader, A., Abdelmasseh, M., Abd-Elsalam, S., Abdi, P., Abdollahi, M., Abdoun, M., Abdullahi, A., Abebe, M., Abiodun, O., Aboagye, R. G.,...Murray, C. J. L. (2024). Burden of disease scenarios for 204 countries and territories, 2022–2050: a forecasting analysis for the Global Burden of Disease Study 2021. The Lancet, 403(10440), 2204-2256. https://doi.org/10.1016/S0140-6736(24)00685-8

Vos, T., Lim, S. S., Abbafati, C., Abbas, K. M., Abbasi, M., Abbasifard, M., Abbasi-Kangevari, M., Abbastabar, H., Abd-Allah, F., Abdelalim, A., Abdollahi, M., Abdollahpour, I., Abolhassani, H., Aboyans, V., Abrams, E. M., Abreu, L. G., Abrigo, M. R. M., Abu-Raddad, L. J., Abushouk, A. I.,...Murray, C. J. L. (2020). Global burden of 369 diseases and injuries in 204 countries and territories, 1990–2019: a systematic analysis for the Global Burden of Disease Study 2019. The Lancet, 396(10258), 1204-1222. https://doi.org/10.1016/S0140-6736(20)30925-9

Zheng, P., Afshin, A., Biryukov, S., Bisignano, C., Brauer, M., Bryazka, D., Burkart, K., Cercy, K. M., Cornaby, L., Dai, X., Dirac, M. A., Estep, K., Fay, K. A., Feldman, R., Ferrari, A. J., Gakidou, E., Gil, G. F., Griswold, M., Hay, S. I.,...Murray, C. J. L. (2022). The Burden of Proof studies: assessing the evidence of risk. Nature Medicine, 28(10), 2038-2044. https://doi.org/10.1038/s41591-022-01973-2